

MULTIGROUP SPACE DEPENDENT NUCLEAR REACTOR  
TRANSIENTS BY CLOSED-FORM ANALYSIS

by

KELVIN F.T. TSE, B.ENG. (McMaster)

PART B: ON-CAMPUS PROJECT\*

A project report submitted in partial fulfillment of the  
requirements for the degree of  
Master of Engineering

Dept. of Engineering Physics

McMaster University

Hamilton, Ontario

February, 1976

\*One of two project reports: The other part is designated PART A:  
McMASTER (Off-Campus) PROJECT.

MASTER OF ENGINEERING (1975)  
Department of Engineering Physics

MCMASTER UNIVERSITY  
Hamilton, Ontario

TITLE: MULTIGROUP SPACE DEPENDENT NUCLEAR REACTOR TRANSIENTS BY  
CLOSED-FORM ANALYSIS

AUTHOR: Kelvin F.T. Tse, B.Eng. (McMaster)

SUPERVISOR: Dr. A.A. Harms

NUMBER OF PAGES: vi, 65

## ABSTRACT

The solution formalism of the closed-form analysis for nuclear reactor transients is investigated in this study. This method of analysis is applied to two one-dimensional test problems, namely, (1) a homogeneous slab and (2) a space dependent problem of the CANDU type. The numerical results have identified some of the characteristics as well as the numerical difficulties associated with the closed-form analysis. Some possible areas for improvements and modifications to the method are suggested.

## ACKNOWLEDGEMENTS

I wish to thank my supervisor, Dr. A.A. Harms, for his valuable guidance and suggestions throughout the course of this project. I also wish to thank Dr. W.J. Garland for the helpful discussions I had with him on many occasions. Finally, a sincere thanks to Mrs. L. Mogensen for the typing of the report.

## LIST OF FIGURES

<u>Figure</u>		<u>Page</u>
1	Neutron flux at slab midplane versus time for four values of reactivity.	28
2	Initial flux distribution.	31

## LIST OF TABLES

<u>Table</u>		<u>Page</u>
1	Flux at slab midplane versus time for four values of reactivity.	29
2	Steady-state pseudo-bucklings.	32
3	Peak thermal flux at $x = 210$ cm versus time.	35

## TABLE OF CONTENTS

	<u>Page</u>
ABSTRACT	iii
ACKNOWLEDGMENTS	iv
LIST OF FIGURES	v
LIST OF TABLES	vi
CHAPTER 1: INTRODUCTION	1
1.1 Purpose of this Project	1
1.2 Reactor Dynamics	1
1.3 The Space Dependent Reactor Kinetics Equations	2
1.4 A Review of Solution Techniques	6
1.4.1 Finite Difference Methods	6
1.4.2 Point Kinetics	7
1.4.3 Modal Expansion Approximations	8
1.4.4 Nodal Approximation	9
CHAPTER 2: A CLOSED-FORM ANALYSIS	11
2.1 Solution Formalism	11
2.2 The Steady-State Case	19
2.3 The Time-Dependent Case	23
CHAPTER 3: NUMERICAL ANALYSIS	26
3.1 Bare Homogeneous Slab	26
3.2 One-Dimensional Space Dependent Problem	27
CHAPTER 4: CONCLUSIONS AND RECOMMENDATIONS	36
APPENDIX A: TEST PROBLEM DATA	38
A.1 Homogeneous Slab	38
A.2 Six-Region Space Dependent Problem	39

	<u>Page</u>
APPENDIX B: USER DESCRIPTION	41
B.1 Program CANDU	41
B.2 Subroutine MAIN	41
B.3 Subroutine STEDY	42
B.4 Subroutine COEMAT	42
B.5 Subroutine RITE	42
B.6 Input Instructions	42
APPENDIX C: PROGRAM LISTING	45
REFERENCES:	64

## CHAPTER 1

### INTRODUCTION

#### 1.1 Purpose of This Project

In large nuclear reactors, localized changes in material compositions cause changes in neutron flux which contribute to changes in power density. The effects of a change in reactivity depend on the size, shape and location of the core region where the reactivity is introduced, as well as on the magnitude of the change. Hence, multidimensional and space dependent reactor kinetics analyses are required to fully describe the effects of a reactivity change.

Various methods of analysis for space dependent reactor kinetics have been published in the literature in past years. One of these is the closed-form analysis, Though not without its limitations, it is particularly simple to apply. The method has been applied by Garland and Harms<sup>(1)</sup> to obtain solutions for the space and time dependent temperature distribution in a cylindrical reactor fuel pin using one neutron group. The purpose of this project is to investigate the feasibility of applying this closed-form analysis to transient flux calculations for a general multiregion reactor.

#### 1.2 Reactor Dynamics

The study of reactor dynamics is concerned with the various aspects of the time dependent behaviour of the core. It includes all

the considerations of coolant flow, heat transfer, fuel behaviour, transients and stability and control. During its course of operation, a reactor's properties may change with time, resulting in a change in the neutron multiplication factor and hence the neutron population. In terms of reactivity, it means that the reactor is disturbed from its critical state. Since a change in neutron population has immediate effects on the power density, the reactor transient behaviour must be accurately determined in order to adequately control the power level.

Changes in reactor properties can occur in many ways. Slow transients or long term effects are associated with such parameters as fuel burnup and Xenon effects. These phenomena, while operationally important, do not present serious safety problems. Fast transients or short term effects may result from temperature changes, prescribed reactivity changes introduced by control rod motion, or accidental changes such as those induced by a loss of coolant. If the reactivity change exceeds a certain level, then the reactor becomes prompt critical, making it very difficult to control and resulting in dangerous operation. It is to these fast transients that reactor dynamics and safety studies are intimately related. With the present generation of power reactors getting increasingly larger, multidimensional space dependent kinetics analyses are necessary to account for the spatially decoupling effects.

### 1.3 The Space Dependent Reactor Kinetics Equations

A rigorous treatment of nuclear reactor kinetics would invoke

energy dependent neutron transport theory. However, a detailed description of the time and spatial behaviour of the neutron population is almost impossible because of the large number of spatially distinct regions and with neutrons travelling in all directions at speeds which span about eight orders of magnitude. Furthermore, the continuously changing core properties have to be taken into consideration simultaneously with neutron effects. However, it has been found by experience that the group diffusion approximation suffices to describe the neutron population in a large number of reactor types.

The time dependent group diffusion equations describe the average reaction rate of neutrons over an interval of energy referred to as a group according to neutron diffusion theory. The space dependent reactor kinetics equations can be written in the following multigroup diffusion approximation form:

$$\frac{1}{V_g} \frac{\partial}{\partial t} \phi_g(\bar{r}, t) = \bar{\nabla} \cdot D_g(\bar{r}, t) \bar{\nabla} \phi_g(\bar{r}, t) + \sum_{g'=1}^G \Sigma_{gg'}(\bar{r}, t) \phi_{g'}(\bar{r}, t) + \sum_{i=1}^I f_{gi} C_i(\bar{r}, t) \quad , \quad (1 \leq g \leq G) \quad (1.1)$$

$$\frac{\partial}{\partial t} C_i(\bar{r}, t) = -\lambda_i C_i(\bar{r}, t) + \sum_{g=1}^G P_{ig}(\bar{r}, t) \phi_g(\bar{r}, t) \quad . (1 \leq i \leq I) \quad (1.2)$$

Parameters appearing in the above equations have the following meanings:

$g$  = index number of the energy group

$i$  = index number of the delayed neutron precursor group

$G$  = total number of energy groups

$I$  = total number of delayed neutron precursor groups

$\phi_g$  = scalar neutron flux [ $n/(cm^2\text{-sec})$ ] in energy group  $g$

$C_i$  = concentration ( $cm^{-3}$ ) of  $i^{\text{th}}$  precursor

$D_g$  = diffusion coefficient (cm) for neutrons in energy group  $g$

$v_g$  = speed (cm/sec) of neutrons in energy group  $g$

$\Sigma_{gg'}$  = intergroup macroscopic transfer cross section ( $cm^{-1}$ ) from group  $g'$  to group  $g$  with the following structure:

$$\Sigma_{gg} = \chi_g(1-\beta)v_g\Sigma_{fg} - \Sigma_{ag} - \sum_{g' \neq g} \Sigma_{g \rightarrow g'}$$

$\chi_g$  = fission spectrum yield in group  $g$

$\nu_g$  = average number of neutrons per fission in group  $g$

$\Sigma_{fg}$  = macroscopic fission cross section ( $cm^{-1}$ ) in group  $g$

$\Sigma_{ag}$  = macroscopic absorption cross section ( $cm^{-1}$ ) in group  $g$

$\Sigma_{g \rightarrow g'}$  = macroscopic scattering cross section from group  $g$  to group  $g'$

$\beta$  = total fractional yield of delayed neutrons per fission

$$\Sigma_{gg'} = \chi_g(1-\beta)v_{g'}\Sigma_{fg'} + \Sigma_{g' \rightarrow g}$$

$f_{gi} = \lambda_i \chi_{gi}$  = probability ( $sec^{-1}$ ) that the  $i^{\text{th}}$  precursor will yield a neutron in group  $g$  where  $\lambda_i$  is the decay constant and  $\chi_{gi}$  the fraction of decays in delayed group  $i$  which yield neutrons in group  $g$

$P_{ig'} = \beta_i v_{g'} \Sigma_{fg'}$  = production factor ( $cm^{-1}$ ) for the  $i^{\text{th}}$  precursor having fractional yield  $\beta_i$  by fissions in group  $g'$ .

Equations (1.1) and (1.2) are coupled partial and ordinary differential equations respectively in which the coefficients are time

dependent. Because of the time dependence of the cross sections, the system actually represents a non-linear set of partial differential equations. However, changes in material properties due to fission heating are so much slower than changes in neutron flux that the coefficients can be considered time independent within the small time interval considered. Of course, changes in cross sections effected by control rod motion or other reactor control actions must be taken into consideration. The space dependent reactor kinetics equations must be solved subject to boundary conditions of the homogeneous Neumann or Dirichlet type. The Neumann boundary condition requires that the neutron current be continuous at internal interfaces  $\bar{r}$  of the reactor at all times,

$$D_g(\bar{r}_+) \bar{\nabla} \phi_g(\bar{r}_+, t) = D_g(\bar{r}_-) \bar{\nabla} \phi_g(\bar{r}_-, t) \quad . \quad (1.3)$$

The Dirichlet boundary conditions specify that the neutron flux vanishes at the extrapolated reactor boundary  $\bar{R}$  and be continuous everywhere within the reactor at all times,

$$\phi_g(\bar{R}, t) = 0 \quad , \quad (1.4)$$

$$\phi_g(\bar{r}_+, t) = \phi_g(\bar{r}_-, t) \quad . \quad (1.5)$$

The initial flux and precursor distributions in space and energy must be specified.

Various solution techniques have been used to approximate the

spatial derivative and/or time derivative of the flux and precursor concentrations to reduce Equations (1.1) and (1.2) to coupled ordinary differential equations or inhomogeneous algebraic equations in the unknowns  $\phi_g$  and  $C_i$ . The following section presents a review of the methods for reactor transient analyses.

#### 1.4 A Review of Solution Techniques

The solution techniques for solving the space dependent multi-group reactor kinetics equations can be divided into two broad categories known as direct methods and indirect methods. The direct methods solve the neutron diffusion equations by finite differencing the equations in space and time. The indirect methods involve some assumption about the shape of the solution over several subregions or the entire reactor and proceed to solve the equations by expanding the solution as a linear combination of some set of functions. Some of these methods are briefly described here.

##### 1.4.1 Finite Difference Methods (2,3,4,5,6)

To obtain the finite difference approximations, the reactor model is partitioned into a finite number of elemental regions or mesh cells, with each cell enclosing a mesh point. The space dependent reactor kinetics equations are then discretized in the spatial variable by integrating the equations over the volume of the reactor, using the box integration technique and replacing the spatial derivative with a finite difference approximation. Likewise, the time derivative is also

replaced by a finite difference to reduce the equations to a set of inhomogeneous algebraic equations, the solutions of which are the neutron flux  $\phi_g(\vec{r}, t)$  and precursor concentration  $C_i(\vec{r}, t)$  at each mesh point. Within the framework of finite difference methods, different techniques have been employed to reduce computation time or to overcome numerical instability problems, with varying degrees of success. These techniques include the alternating direction implicit methods,<sup>(3)</sup> ADI, and alternating direction explicit methods, ADE.<sup>(4)</sup> In finite difference methods, it has been found that applying a group-dependent frequency transformation<sup>(3)</sup> or a characteristic frequency transformation to all groups<sup>(4)</sup> would speed up the convergence rate of the solution. Harms et al. have also demonstrated that the multiple temporal-mode transformation technique is capable of generating very accurate solutions.<sup>(6)</sup>

All finite difference methods have the advantage that definite error bounds on the final approximation can be established. However, to adequately describe the spatial details of a reactor, a large number of mesh points are required. Thus, these methods are as yet considered too expensive for routine production calculations.

#### 1.4.2 Point Kinetics<sup>(7,8)</sup>

In the most common application of the point kinetics approximation, a fixed spatial distribution is assumed. The neutron flux is represented as a product of a time-independent shape function  $\psi_g(\vec{r})$  and an amplitude function  $N_g(t)$ ,

$$\phi_g(\bar{r}, t) \longrightarrow \psi_g(\bar{r})N_g(t) \quad . \quad (1.6)$$

If it is assumed that the amplitude function has an exponential time dependence  $e^{\omega t}$ , then the transient neutron flux is fixed in shape but is varying in amplitude. Space-time effects can be incorporated into the point kinetics model by quasistatic methods or adiabatic methods, which recompute the point kinetics parameters periodically to account for spatial flux tilts. The point kinetics model is a simple method for obtaining only the total power or neutron flux level in the reactor.

#### 1.4.3 Modal Expansion Approximations (7)

One type of modal expansion approximations is the time-synthesis method. In this method, the neutron flux is expanded in known functions  $\psi_{gn}(\bar{r})$  with unknown expansion coefficients  $a_{gn}(t)$ :

$$\phi_g(\bar{r}, t) \approx \sum_{n=1}^N \psi_{gn}(\bar{r})a_{gn}(t) \quad . \quad (1.7)$$

The above approximation is substituted into Equations (1.1) and (1.2). The spatial derivative in Equations (1.1) and (1.2) is eliminated when these equations are premultiplied by some weighting functions and integrated over the entire spatial domain. Thus, the neutron and precursor balance equations are satisfied, not at each spatial point, but in a weighted integral sense over the spatial domain for  $N$  different weighting functions.

Another type of modal expansion approximations is the space-time synthesis method which expands the flux in the following form:

$$\phi_g(\bar{r}, t) = \sum_{n=1}^N \psi_{gn}(x, y) a_{gn}(z, t) \quad (1.8)$$

The same "substitute, weight and integrate" procedure is followed to obtain a set of ordinary differential equations in the time variable, but the weighting functions and the integration involve only two of the spatial variables while the expansion coefficients are functions of the remaining spatial variable as well as of time.

In applying the modal expansion approximations, the choice of expansion functions and weighting functions is of extreme importance for accurate results. One method of choosing the expansion functions is to use eigenfunctions of the Helmholtz equation which for regular geometries are analytical functions.

#### 1.4.4 Nodal Approximation <sup>(7)</sup>

In applying the nodal approximation, the reactor model is divided into a small number of regions. Associated with each region is a node. The neutron flux within each node  $R_j$  is written as the product of a shape function  $\psi_{gj}(\bar{r})$  and an amplitude function  $N_{gj}(t)$ :

$$\phi_g(\bar{r}, t) = \psi_{gj}(\bar{r}) N_{gj}(t) \quad \bar{r} \in R_j \quad (1.9)$$

The above relation is substituted into Equations (1.1) and (1.2) which are then multiplied by appropriate weighting functions and integrated over the volume of region  $j$ . Whereas the modal expansion approximations are capable of predicting the transient neutron flux at each point, the nodal approximation is oriented towards obtaining the average flux in

each region of the reactor.

In the following chapter, the method of closed-form analysis is described.

## CHAPTER 2

### A CLOSED-FORM ANALYSIS

The previous sections have reviewed some of the commonly used techniques for nuclear reactor transient analyses. As mentioned in the introduction, an alternative solution technique, the closed-form method, has been applied by Garland and Harms<sup>(1)</sup> to time dependent temperature distribution calculation in a cylindrical fuel pin. The objective of this project is to investigate the possible extension of this method to transient flux calculations. The formalism of this solution technique is presented in the following section.

#### 2.1 Solution Formalism

The starting point for this analysis is the space dependent reactor kinetics equations, Eq. (1.1) and (1.2), which are rewritten here for the sake of clarity,

$$\begin{aligned} \frac{1}{v_g} \frac{\partial}{\partial t} \phi_g(\vec{r}, t) = & \bar{\nabla} \cdot D_g(\vec{r}, t) \bar{\nabla} \phi_g(\vec{r}, t) + \sum_{g'=1}^G \Sigma_{gg'}(\vec{r}, t) \phi_{g'}(\vec{r}, t) \\ & + \sum_{i=1}^I f_{gi} C_i(\vec{r}, t), \quad (1 \leq g \leq G) \end{aligned} \quad (2.1)$$

$$\frac{\partial}{\partial t} C_i(\vec{r}, t) = -\lambda_i C_i(\vec{r}, t) + \sum_{g'=1}^G P_{ig'}(\vec{r}, t) \phi_{g'}(\vec{r}, t). \quad (1 \leq i \leq I) \quad (2.2)$$

The symbols in these equations have previously been defined in Section 1.3. For convenience in later discussion, Equations (2.1) and (2.2) are combined in the following compact matrix form:

$$\frac{\partial}{\partial t} \bar{\Phi}(\bar{r}, t) = \underline{M}(\bar{r}, t) \bar{\Phi}(\bar{r}, t) \quad . \quad (2.3)$$

Here,  $\bar{\Phi}$  is a vector of length  $N$  representing the neutron flux or precursor concentration at a point  $\bar{r}$ ,

$$\bar{\Phi}(\bar{r}, t) = \begin{bmatrix} \phi_1(\bar{r}, t) \\ \phi_2(\bar{r}, t) \\ \vdots \\ \phi_G(\bar{r}, t) \\ c_1(\bar{r}, t) \\ \vdots \\ c_I(\bar{r}, t) \end{bmatrix} = \begin{bmatrix} \Phi_1(\bar{r}, t) \\ \Phi_2(\bar{r}, t) \\ \vdots \\ \Phi_G(\bar{r}, t) \\ \Phi_{G+1}(\bar{r}, t) \\ \vdots \\ \Phi_N(\bar{r}, t) \end{bmatrix} \quad , \quad (2.4)$$

where  $N$  is the total number of neutron and delayed precursor groups.

$\underline{M}(\bar{r}, t)$  is an operator matrix of order  $N$ :

$$\underline{M}(\bar{r}, t) = \begin{bmatrix} v_1(\bar{\nabla} \cdot D_1 \bar{\nabla} + \Sigma_{11}) & v_1 \Sigma_{12} & v_1 \Sigma_{1G} & v_1^f{}_{11} & \cdots & v_1^f{}_{1I} \\ v_2 \Sigma_{21} & v_2(\bar{\nabla} \cdot D_2 \bar{\nabla} + \Sigma_{22}) & \cdots & v_2 \Sigma_{2G} & v_2^f{}_{21} & \cdots & v_2^f{}_{2I} \\ \cdot & \cdot & \cdot & \cdot & \cdot & \cdot & \cdot \\ v_G \Sigma_{G1} & v_G \Sigma_{G2} & \cdots & v_G(\bar{\nabla} \cdot D_G \bar{\nabla} + \Sigma_{GG}) & v_G^f{}_{G1} & \cdots & v_G^f{}_{GI} \\ P_{11} & P_{12} & \cdots & P_{1G} & -\lambda_1 & \cdots & \underline{0} \\ \cdot & \cdot & \cdot & \cdot & \cdot & \cdot & \cdot \\ \cdot & \cdot & \cdot & \cdot & \cdot & \cdot & \underline{0} \\ P_{I1} & P_{I2} & \cdots & P_{IG} & \cdots & \cdots & -\lambda_I \end{bmatrix} \quad (2.5)$$

In an attempt to combine space dependent with space independent solutions, the general solution representation is written as

$$\phi_n(\bar{r}, t) = H_n \psi(\bar{r}, t) + \sum_{j=1}^N E_{nj} e^{\omega_j t}, \quad (1 \leq n \leq N) \quad (2.6)$$

where  $H_n$  and  $E_{nj}$  are group dependent coefficients to be determined.

The choice of a summation of  $N$  terms for the space independent solution will become clear later on. In both the time-synthesis method and point kinetics analysis, separation of the flux in space and time is assumed. Here, separation of variables is also assumed for the space dependent solution  $\psi(\bar{r}, t)$ ,

$$\psi(\bar{r}, t) \longrightarrow R(\bar{r})T(t) \longrightarrow X(r_1)Y(r_2)Z(r_3)T(t), \quad (2.7)$$

where  $r_1$ ,  $r_2$ , and  $r_3$  represent the spatial variables involved in a three-dimensional case. In Eq. (2.6), the addition of the space independent part is intended to remove the limitations imposed by the separation of space and time procedure on the magnitude of the transient to be examined.

Substituting Eq. (2.6) into Equations (2.1) and (2.2), the resulting equations can be separated into space dependent and space independent parts, and are written as:

Space dependent part:

$$\begin{aligned} \frac{1}{v_g} H_g \frac{\partial}{\partial t} \psi(\bar{r}, t) &= H_g \bar{\nabla} \cdot D_g(\bar{r}) \bar{\nabla} \psi_g(\bar{r}, t) + \sum_{g'=1}^G \Sigma_{gg'}(\bar{r}, t) H_{g'} \psi(\bar{r}, t) \\ &+ \sum_{i=1}^I f_{gi} H_{G+i} \psi(\bar{r}, t) \quad , \quad (1 \leq g \leq G) \end{aligned} \quad (2.8)$$

$$H_{G+i} \frac{\partial}{\partial t} \psi(\bar{r}, t) = -\lambda_i H_{G+i} \psi(\bar{r}, t) + \sum_{g'=1}^G P_{ig'}(\bar{r}, t) H_{g'} \psi(\bar{r}, t) \quad ,$$

$$(1 \leq i \leq I) \quad (2.9)$$

Space independent part:

$$\begin{aligned} \frac{1}{v_g} \sum_{j=1}^N E_{gj} \omega_j e^{\omega_j t} &= \sum_{g'=1}^G \Sigma_{gg'}(\bar{r}, t) \sum_{j=1}^N E_{g'j} e^{\omega_j t} \\ &+ \sum_{i=1}^I f_{gi} \sum_{j=1}^N E_{G+i,j} e^{\omega_j t} \quad , \quad (1 \leq g \leq G) \end{aligned} \quad (2.10)$$

$$\sum_{j=1}^N E_{G+i,j} \omega_j e^{\omega_j t} = -\lambda_i \sum_{j=1}^N E_{G+i,j} e^{\omega_j t} + \sum_{g'=1}^G P_{ig'}(\vec{r}, t) \sum_{j=1}^N E_{g',j} e^{\omega_j t} \quad (1 \leq i \leq I) \quad (2.11)$$

Equations (2.8) and (2.9) for the space dependent solutions can be written in the following form:

$$\left\{ \frac{\partial}{\partial t} \psi(\vec{r}, t) \right\} \bar{H} = \underline{M}(\vec{r}, t) \cdot \psi(\vec{r}, t) \underline{I} \cdot \bar{H} \quad , \quad (2.12)$$

where  $\bar{H}$  is a vector of length  $N$  containing the coefficients  $H_n$ ,  
 $1 \leq n \leq N$ ,

$$\bar{H} = \begin{bmatrix} H_1 \\ H_2 \\ \vdots \\ H_N \end{bmatrix} \quad , \quad (2.13)$$

and  $\underline{M}(\vec{r}, t)$  is the system operator matrix previously defined in Eq. (2.5).

For a homogeneous region, the cross sections and the diffusion coefficients can be considered space independent within that region. Assuming separation of variables, Eq. (2.7), and assuming that the spatial dependence of  $\psi(\vec{r}, t)$  is governed by the solution to the Helmholtz equation,

$$\nabla^2_R(\vec{r}) = -B^2_R(\vec{r}) \quad , \quad (2.14)$$

then Eq. (2.12) can be written as

$$\{R(\bar{r}) \frac{dT(t)}{dt}\} \bar{H} = R(\bar{r}) T(t) \underline{A} \bar{H}, \quad (2.15)$$

where  $\underline{A}$  is a system coefficient matrix of order  $N$ ,

$$\underline{A} = \begin{bmatrix} v_1(-D_1 B^2 + \Sigma_{11}) & v_1 \Sigma_{12} & \dots & v_1 \Sigma_{1G} & v_1 f_{11} \dots v_1 f_{1I} \\ v_2 \Sigma_{21} & v_2(-D_2 B^2 + \Sigma_{22}) & \dots & v_2 \Sigma_{2G} & v_2 f_{21} \dots v_2 f_{2I} \\ \cdot & \cdot & \cdot & \cdot & \cdot \\ v_G \Sigma_{G1} & v_G \Sigma_{G2} & \dots & v_G(-D_G B^2 + \Sigma_{GG}) & v_G f_{G1} \dots v_G f_{GI} \\ P_{11} & P_{12} & \dots & P_{1G} & -\lambda_1 \\ \cdot & \cdot & \cdot & \cdot & \cdot \\ P_{I1} & P_{I2} & \dots & P_{IG} & -\lambda_I \end{bmatrix} \quad (2.16)$$

The matrix  $\underline{A}$  differs from the matrix  $\underline{M}$  in that the spatial derivative operator in Eq. (2.8) is now replaced by the buckling  $B^2$ .

Equation (2.15) can be written as follows:

$$\frac{1}{T(t)} \frac{dT(t)}{dt} \bar{H} = \underline{A} \bar{H} \quad (2.17)$$

If it is further assumed that the time dependence is of the exponential form  $e^{\delta t}$ , then Eq. (2.17) can be written as

$$(\underline{A} - \delta \underline{I}) \bar{H} = 0 \quad (2.18)$$

Equation (2.18) actually represents a system of eigenfunction equations. The  $\delta$ 's are given by the eigenvalues and the coefficients  $H_n$  are given by the eigenvectors. For a system with a total of  $N$  energy and delayed precursor groups, there are  $N$  eigenvalues and  $N$  eigenvectors. Thus the space dependent solution in Eq. (2.6) can be represented as

$$H_n \psi(\bar{r}, t) \longrightarrow R(B, \bar{r}) \sum_{j=1}^N H_{nj} e^{\delta_j t}, \quad (1 \leq n \leq N) \quad (2.19)$$

where  $R(B, \bar{r})$  can be considered as the shape function and is given as a solution to the Helmholtz equation, Eq. (2.14). Hence, the shape function  $R(B, \bar{r})$  is dependent on the buckling  $B^2$ . It should be pointed out that the eigenvectors  $H_{nj}$  obtained from Eq. (2.18) are not normalized. They can be normalized by considering the boundary conditions at  $t = 0$ . The application of these boundary conditions leads to transcendental equations which can be solved by matrix analysis, as will be shown in Section 2.3.

As can be seen from Eq. (2.18), all the elements of the system coefficient matrix  $\underline{A}$  must be known before the eigenvalues  $\delta_j$  and the eigenvectors  $H_{nj}$  can be determined. The reactor material constants are of course assumed known, but the buckling  $B^2$  has yet to be specified. In this analysis, the steady-state pseudo-bucklings are assumed throughout the transient. The determination of the steady-state pseudo-bucklings will be described in Section 2.2.

So far only the space dependent solution has been considered. The treatment of the space independent solution is described in what follows. It can be seen that the space independent solution is obtained

in a manner similar to that for the space dependent solution.

All expressions in Equations (2.10) and (2.11) for the space independent part contain a summation of terms over  $j$ ,  $1 \leq j \leq N$ . Thus, taking the  $j^{\text{th}}$  term in each expression, the resulting equations can be written as

$$\begin{aligned} \frac{1}{v_g} E_{gj} \omega_j e^{\omega_j t} &= \sum_{g'=1}^G \Sigma_{gg'}(\bar{r}, t) E_{g'j} e^{\omega_j t} \\ &+ \sum_{i=1}^I f_{gi} E_{G+i,j} e^{\omega_j t}, \quad (1 \leq g \leq G) \end{aligned} \quad (2.20)$$

$$\begin{aligned} E_{G+i,j} \omega_j e^{\omega_j t} &= -\lambda_i E_{G+i,j} e^{\omega_j t} \\ &+ \sum_{g'=1}^G P_{ig'}(\bar{r}, t) E_{g'j} e^{\omega_j t}. \quad (1 \leq i \leq I) \end{aligned} \quad (2.21)$$

Equations (2.20) and (2.21), after dividing by  $e^{\omega_j t}$ , can be combined into the following matrix form,

$$\underline{A}'(\bar{r}, t) \bar{E}_j = \omega_j \bar{E}_j. \quad (2.22)$$

Here,  $\underline{A}'$  is a coefficient matrix of order  $N$ . It differs from the  $\underline{A}$  matrix in Eq. (2.16) in that there are no leakage terms,  $-D_g B^2$ , along the diagonal.  $\bar{E}_j$  is a vector of length  $N$  containing the  $j^{\text{th}}$  term of each energy and delayed precursor group. Equation (2.22), like Eq. (2.18), also represents a system of eigenfunction equations. Thus it can be seen

that the space independent solution representation in Eq. (2.6) is consistent. Since all the elements of the matrix  $\underline{A}^t$  are known, the  $\omega_j$ 's are given by the eigenvalues and the coefficients  $E_{nj}$  by the eigenvectors. The coefficients  $E_{nj}$  can be normalized by considering the initial conditions  $\phi_n(\bar{r}, 0)$  at  $t = 0$ . Again, these conditions lead to transcendental equations.

## 2.2 The Steady-State Case

The steady-state neutron diffusion equations are written as follows:

$$0 = \bar{\nabla} \cdot D_g(\bar{r}) \bar{\nabla} \phi_g(\bar{r}) - \Sigma_{ag}(\bar{r}) \phi_g(\bar{r}) + \chi_g \sum_{g'=1}^G \nu \Sigma_{fg'}(\bar{r}) \phi_{g'}(\bar{r}) + \sum_{g' \neq g} \Sigma_{g' \rightarrow g}(\bar{r}) \phi_{g'}(\bar{r}), \quad (1 \leq g \leq G) \quad (2.23)$$

$$C_i(\bar{r}) = \frac{\beta_i}{\lambda_i} \sum_{g'=1}^G \nu \Sigma_{fg'}(\bar{r}) \phi_{g'}(\bar{r}). \quad (1 \leq i \leq I) \quad (2.24)$$

The symbols in Equations (2.23) and (2.24) have previously been defined in Section 1.3. In the steady-state case, the time dependence in the solution representation is suppressed. Thus, the group  $g$  flux may be written as

$$\phi_g(\bar{r}) = H_g \psi(\bar{r}) + \sum_{j=1}^N E_{gj} \quad (2.25)$$

Substituting Eq. (2.25) into Eq. (2.23), the resulting equations can be separated into space dependent and space independent parts. With the assumption that the space dependence is governed by the Helmholtz equation, Eq. (2.14), the space dependent part for group  $g$  within a homogeneous region is written as

$$0 = -D_g B^2 H_g \psi(\vec{r}) - \Sigma_{ag} H_g \psi(\vec{r}) + \chi_g \sum_{g'=1}^G \nu \Sigma_{fg'} H_{g'} \psi(\vec{r}) + \sum_{g' \neq g} \Sigma_{g' \rightarrow g} H_{g'} \psi(\vec{r}) \quad (1 \leq g \leq G) \quad (2.26)$$

The  $G$  equations for  $G$  energy groups can be combined in the following matrix form,

$$\underline{F} \underline{H} = 0 \quad , \quad (2.27)$$

where  $\underline{F}$  is a matrix of order  $G$ ,

$$\underline{F} = \begin{bmatrix} -D_1 B^2 + \Sigma_{11} & \Sigma_{12} & \dots & \Sigma_{1G} \\ \Sigma_{21} & -D_2 B^2 + \Sigma_{22} & \dots & \Sigma_{2G} \\ \cdot & \cdot & \cdot & \cdot \\ \Sigma_{G1} & \Sigma_{G2} & \dots & -D_G B^2 + \Sigma_{GG} \end{bmatrix} \quad , \quad (2.28)$$

and  $\underline{H}$  is redefined as

$$\bar{H} = \begin{bmatrix} H_1 \\ H_2 \\ \vdots \\ H_G \end{bmatrix}$$

The requirement for non-zero solutions  $H_g$  is that the determinant of  $\underline{F}$  vanishes. The vanishing determinant gives rise to a polynomial or characteristic equation of degree  $G$  in  $B^2$ . Thus the pseudo-bucklings are given by the  $G$  roots of this characteristic equation. The unknowns  $H_g$  are the eigenvectors of Eq. (2.27) and are given by any non-zero column of the adjoint of  $\underline{F}$  to within arbitrary constants.<sup>(9)</sup> Therefore, in a system with  $G$  energy groups, there are a total of  $G$  pseudo-bucklings,  $B_{g'}^2$ ,  $1 \leq g' \leq G$ . For each  $B_{g'}^2$ , there are two independent solutions to the Helmholtz equation,

$$\psi_{g'}(\bar{r}) = a_{g',1} W_1(B_{g'}, \bar{r}) + a_{g',2} W_2(B_{g'}, \bar{r}) \quad , \quad (1 \leq g' \leq G) \quad (2.29)$$

where  $W_1(B_{g'}, \bar{r})$  and  $W_2(B_{g'}, \bar{r})$  are the independent solutions associated with the  $g'$ <sup>th</sup> eigenmode and  $a_{g',1}$ ,  $a_{g',2}$  are coefficients yet to be determined. Thus the space dependent solution for group  $g$  can be expanded in the following manner,

$$H_g \psi(\bar{r}) \longrightarrow \sum_{g'=1}^G [a_{g',1} W_1(B_{g'}, \bar{r}) + a_{g',2} W_2(B_{g'}, \bar{r})] H_{gg'} \quad . \quad (2.30)$$

The coefficients  $a_{g'1}$  and  $a_{g'2}$  are most conveniently found by considering boundary conditions. It should be pointed out that Eq. (2.30) gives only the flux shape. As previously mentioned, the coefficients  $H_{gg}$ , are determined to within arbitrary constants. However, they can be normalized against the power level within the homogeneous region under consideration.

The space independent part can be treated in a similar manner. After substituting Eq. (2.25) into Eq. (2.23) and equating the  $j^{\text{th}}$  term, the G equations for the space independent part can be put into the following matrix form,

$$\underline{F}' \underline{\bar{E}}_j = 0 \quad , \quad (2.31)$$

where

$$\underline{\bar{E}}_j = \begin{bmatrix} E_{1j} \\ E_{2j} \\ \vdots \\ E_{Gj} \end{bmatrix} \quad , \quad (2.32)$$

and  $\underline{F}'$  differs from  $\underline{F}$  in Eq. (2.28) in that the diagonal elements do not contain the leakage terms. Again, for non-zero  $E_{gj}$ , it is required that the determinant of  $\underline{F}'$  vanishes. However, because of the condition already imposed on the space dependent part, i.e.,

$$\det \underline{F} = 0 \quad , \quad (2.33)$$

the requirement for the space independent part is not satisfied. Thus, all the coefficients  $E_{gj}$  are equal to zero. Therefore, in the steady-state case, the space independent part in Eq. (2.25) is not included in the final solution representation. However, it may be included in the analysis for the transient case, as will be shown in the following section.

### 2.3 The Time Dependent Case

Now that the steady-state pseudo-bucklings have been determined, they can be used to approximate the spatial derivative in Eq. (2.8). Thus, for each value of  $B_{g_i}^2$ , Eq. (2.18) becomes

$$(\underline{A}_{g_i} - \delta_{g_i} \underline{I}) \bar{H}_{g_i} = 0 \quad . \quad (2.34)$$

Here, the  $N$  by  $N$  matrix  $\underline{A}_{g_i}$  is derived from the matrix  $\underline{A}$  in Eq. (2.16), with the term  $B^2$  replaced by  $B_{g_i}^2$ . Similarly,  $\delta_{g_i}$  and  $\bar{H}_{g_i}$  are the eigenvalues and eigenvectors associated with the  $g_i^{\text{th}}$  eigenmode. Therefore, the solution in the time dependent case can be written as

$$\phi_n(\bar{r}, t) = \sum_{g_i=1}^G \{ [a_{g_i,1} W_1(B_{g_i}, \bar{r}) + a_{g_i,2} W_2(B_{g_i}, \bar{r})] \cdot \sum_{j=1}^N H_{ng_i, j} e^{\delta_{g_i, j} t} \} + \sum_{j=1}^N E_{nj} e^{\omega_j t} \quad . \quad (1 \leq n \leq N) \quad (2.35)$$

Here,  $\phi_n(\bar{r}, t)$  represents the group flux for  $1 \leq n \leq G$ , or the delayed neutron precursor concentration for  $G+1 \leq n \leq N$ .  $N$  is the total number of energy and delayed precursor groups. The space dependent solution is

summed over all the eigenmodes, each denoted by the subscript  $g'$ ,  
 $1 \leq g' \leq G$ .

In Eq. (2.35), the coefficients  $a_{g',1}$  and  $a_{g',2}$ , as well as the shape functions  $W_1(B_{g'}, \bar{r})$  and  $W_2(B_{g'}, \bar{r})$ , are obtained from the steady-state solutions. The  $\delta_{g',j}$ 's and  $\omega_j$ 's are given by the eigenvalues of Eq. (2.34) and Eq. (2.22) respectively. Similarly, the coefficients  $H_{ng',j}$  and  $E_{nj}$  are given by the eigenvectors of Eq. (2.34) and Eq. (2.22) respectively and they are determined to within arbitrary constants. These coefficients can be normalized by considering boundary conditions or by equating to initial conditions.

In the multiple temporal-mode transformation analysis by Harms et al., which does not include the space independent solution, the coefficients are normalized to the initial values.<sup>(6)</sup> Thus, along this vein, for the  $g'$ <sup>th</sup> eigenmode solution at the initial time  $t = 0$  of each time interval, we can write

$$\begin{aligned} [a_{g',1}W_1(B_{g'}, \bar{r}) + a_{g',2}W_2(B_{g'}, \bar{r})] \sum_{j=1}^N H_{ng',j} \\ = b_{n1}W_1(B_{g'}, \bar{r}) + b_{n2}W_2(B_{g'}, \bar{r}) \quad , \end{aligned} \quad (2.36)$$

where  $b_{n1}$  and  $b_{n2}$  are the known coefficients determined from the previous time interval. Equation (2.36) provides a normalization condition for the coefficients  $H_{ng',j}$  if no space independent part is considered.

However, if the space independent solution is also included, a different normalization procedure is called for. The approach used in this analysis is described here. First, the coefficients  $E_{nj}$  for the space independent part in each region are normalized against the initial conditions

at one boundary of the region at the initial time  $t = 0$ ,

$$\sum_{j=1}^N E_{nj} = \phi_n(\bar{r}_1, 0) \quad , \quad (2.37)$$

where  $\bar{r}_1$  specifies the position at the region boundary considered. Thus, all the coefficients  $E_{nj}$  are now determined. The normalizing conditions for the coefficients  $H_{ng'j}$  in the space dependent solution are derived by equating Eq. (2.35) to the initial conditions at the region boundaries. However, because of the condition already imposed on the space independent part, Eq. (2.37), the equation obtained for group  $n$  at the region boundary  $\bar{r}_1$  is reduced to

$$\sum_{g'=1}^G [a_{g',1} W_1(B_{g',\bar{r}_1}) + a_{g',2} W_2(B_{g',\bar{r}_1})] \sum_{j=1}^N H_{ng'j} = 0 \quad . \quad (2.38)$$

Equation (2.38) implies that the coefficients  $H_{ng'j}$  are linearly dependent since the expressions

$$[a_{g',1} W_1(B_{g',\bar{r}_1}) + a_{g',2} W_2(B_{g',\bar{r}_1})] \quad ,$$

are not all equal to zero. Therefore, the conditions of continuity of flux and current at time  $t$  at region interfaces must also be utilized to normalize the coefficients  $H_{ng'j}$ . Thus, in theory, all the unknowns in the solution representation, Eq. (2.35), are determined. In Chapter 3, the numerical results of two test problems will be discussed.

## CHAPTER 3

### NUMERICAL ANALYSIS

In this study, the closed-form analysis is tested on two numerical problems. The first case is a homogeneous slab and the second a one-dimensional space dependent problem of the CANDU type. Some of the numerical results are presented in the following sections.

#### 3.1 Bare Homogeneous Slab

Geometry and Composition: Appendix A.1

This test case represents a bare homogeneous slab reactor, 200 cm in width with one energy group and one delayed neutron precursor group. The boundary condition is zero flux on the reactor boundary.

The shape function is given by the solution to the Helmholtz equation, Eq. (2.14), and is a cosine distribution,

$$\psi(x) = a \cos(Bx), \quad (-H \leq x \leq H) \quad (3.1)$$

where  $B^2$  is the buckling and  $H$  is the half-width of the reactor. Only the fundamental mode is considered since for this one-group one-region system, there is no change in flux shape. Thus, the buckling is easily obtained by considering the zero flux boundary condition,

$$B^2 = \left(\frac{\pi}{2H}\right)^2. \quad (3.2)$$

The criticality factor for this system is given by<sup>(8)</sup>

$$k_{\text{eff}} = \frac{\nu \Sigma_f}{\Sigma_a + DB^2} \quad (3.3)$$

In this test problem, the initial configuration was made critical by dividing the fission cross section by the initial critical  $k_{\text{eff}}$ . The initial cosine flux distribution was normalized to unity at the reactor centre plane. The initial delayed neutron precursor concentrations were in equilibrium with the critical flux distribution.

Positive reactivity was introduced to the system by a step decrease in the absorption cross section. Because of the zero flux boundary condition, the space independent solution as mentioned in Eq. (2.6) was not considered. The closed-form analysis used was then similar to the eigenvector expansion technique. The time behaviour of the neutron flux at the reactor midplane for various values of reactivity is shown in Table 1 and Fig. 1. All reactivity values listed here were less than the prompt critical value. Since there is no change in flux shape, Fig. 1 also represents the relative increase in reactor power. The assumption of a constant buckling for this problem was considered satisfactory because of the constant flux shape.

### 3.2 One-Dimensional Space Dependent Problem

Geometry and Composition: Appendix A.2

This test case is a one-dimensional space dependent problem, with two energy groups and two delayed neutron precursor groups. The properties of the model are based on a CANDU type reactor. The reactor model

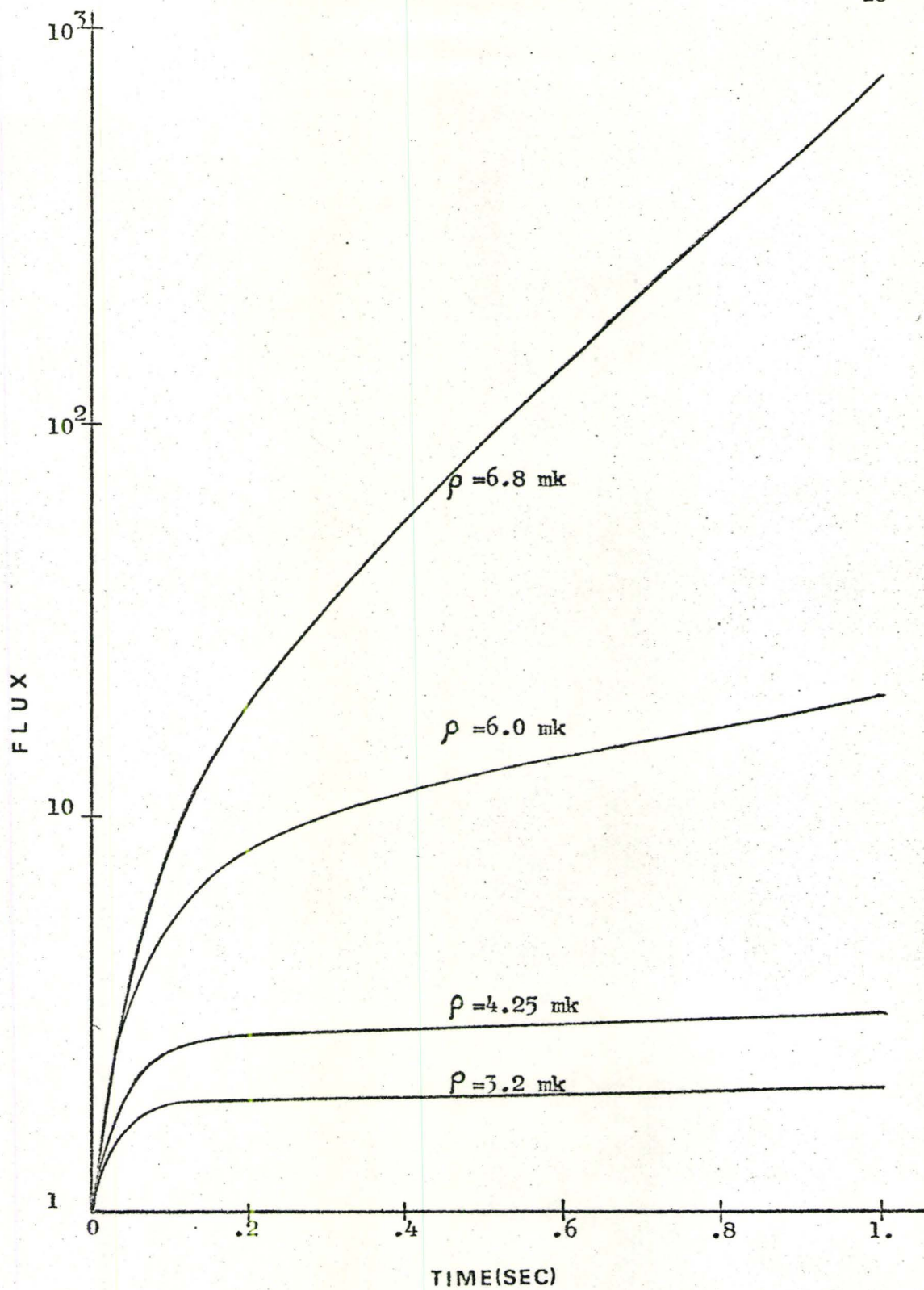


Fig. 1: Neutron flux at slab midplane versus time for four values of reactivity.

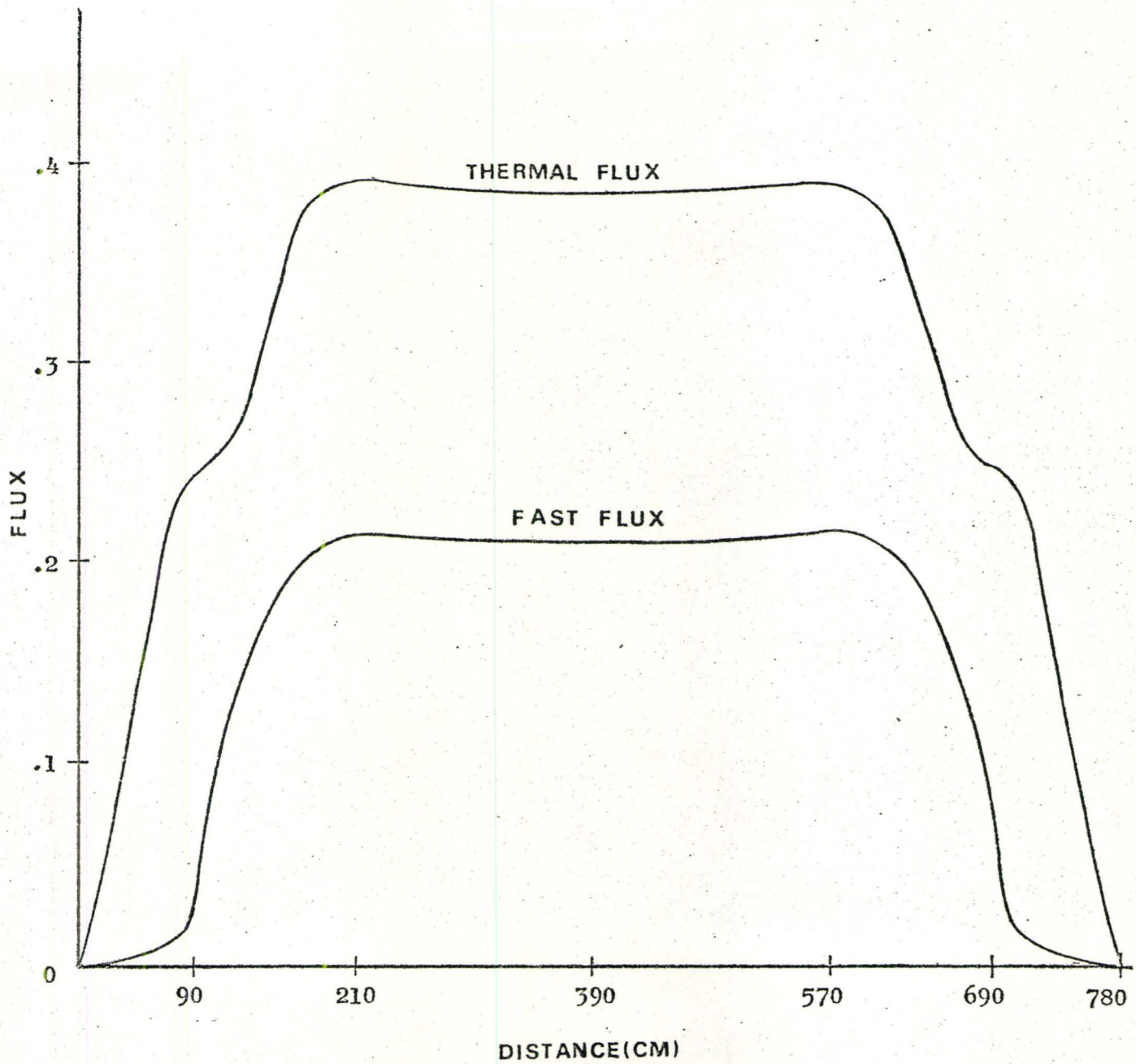
Table 1: Flux at slab midplane versus time for four values of reactivity

Time (sec)	Flux			
	$\rho = 3.2 \text{ mk}$	$\rho = 4.25 \text{ mk}$	$\rho = 6.0 \text{ mk}$	$\rho = 6.8 \text{ mk}$
0.	1.0	1.0	1.0	1.0
.1	1.93	2.70	5.79	9.18
.2	1.97	2.89	8.73	2.05 E1
.3	1.99	2.95	1.07 E1	3.65 E1
.4	2.00	3.00	1.23 E1	5.99 E1
.5	2.02	3.04	1.36 E1	9.43 E1
.6	2.03	3.09	1.49 E1	1.45 E2
.7	2.05	3.13	1.62 E1	2.22 E2
.8	2.07	3.18	1.75 E1	3.36 E2
.9	2.08	3.23	1.89 E1	5.06 E2
1.0	2.10	3.27	2.04 E1	5.75 E2

consists of six regions. Regions 2,3,4 and 5 represent the core and regions 1 and 6 are the reflectors (see Fig. 2).

The initial reactor configuration was made critical by dividing the production cross sections by the initial critical  $k_{\text{eff}}$ , which had been obtained by a finite difference code, ADEP.<sup>(9)</sup> The steady-state flux distribution was obtained by following the procedure outlined in Section 2.2. Figure 2 shows the steady-state fast and thermal flux distributions. These were in close agreement with the ADEP solutions. For this two-group problem, there are two pseudo-bucklings in each region and these are listed in Table 2. The initial precursor concentrations were in equilibrium with the critical flux distribution. The initial reactor power was normalized to unity. The perturbation was introduced by a ramp decrease in the thermal group absorption cross sections in regions 2 and 3 to simulate voiding in one half of the core. The time interval of interest was divided into small steps  $\Delta t$ . The cross sections were considered constant within the time step  $\Delta t$  and were updated at the end of the time step.

In the first attempt to obtain the transient flux solution, the space independent part in Eq. (2.6) was included for consideration. However, for this test problem, the approach outlined in Section 2.3 resulted in numerical difficulties. The normalization conditions for the coefficients  $H_{ng,j}$  resulted in a singularity matrix. This was due to the fact that one of the eigenvalues obtained using the second pseudo-buckling was algebraically much larger than the other eigenvalues. This large eigenvalue was  $\sim .6 \times 10^5$ . Referring to Table 2, it can be seen that, in regions 2,3,4, and 5, the pseudo-buckling for the second eigenmode was



REGIONS



Fig. 2: Initial flux distribution

Table 2: Steady-state pseudo-bucklings

Regions	$B_1^2$	$B_2^2$
1,6	- .7794 E-2	- .2685 E-3
2,5	.7795 E-4	- .1069 E-1
3,4	- .1129 E-5	- .1068 E-1

larger in magnitude than that for the first by an order of 3 to 4. Furthermore, using the second pseudo-buckling, the terms  $D_g B^2$  along the diagonal of the matrix  $\underline{A}_g$ , in Eq. (2.34) were significantly larger than the cross sections which were in the range of  $10^{-4}$  to  $10^{-3}$ . Thus, the resulting eigenvalues for the core were predominantly determined by the pseudo-buckling for the second eigenmode. Since the normalization conditions for the coefficients  $H_{ng'j}$  involved continuity of flux and current at region interfaces at  $t = \Delta t$ , the terms  $e^{\delta_{nj}\Delta t}$  were evaluated. These terms resulted in a singularity matrix which persisted even for small  $\Delta t$ 's in the range of microseconds.

In later attempts to obtain the transient flux solutions, the space independent part was not included in the solution representation and a normalization procedure similar to that for the multiple temporal-mode transformation analysis was adopted. However, the relatively large eigenvalues corresponding to the second eigenmode again resulted in numerical difficulties. In regions 2 and 3, unreasonably large fluxes as well as negative fluxes were obtained. Thus, it can be concluded that the procedure of assuming an exponential time dependence for the second eigenmode was not satisfactory for this test problem.

In the final analysis for this test problem, an exponential time dependence was assumed for only the first eigenmode and no space independent solution was considered. Thus the solution representation used for this problem was

$$\begin{aligned} \Phi_n(\bar{r}, t) = & [a_{11}W_1(B_1\bar{r}) + a_{12}W_2(B_1\bar{r})] \cdot \sum_{j=1}^4 H_{n1j} e^{\delta_{1j}\Delta t} \\ & + [a_{21}W_1(B_2\bar{r}) + a_{22}W_2(B_2\bar{r})]H_{n2} \cdot \quad (1 \leq n \leq N) \end{aligned} \quad (3.4)$$

The following normalization condition was used,

$$\sum_{j=1}^N H_{nj} = 1 \quad (1 \leq n \leq N) \quad (3.5)$$

In Table 3, the peak thermal flux obtained was compared to the ADEP solution for a transient of 0.04 seconds.

Although the peak thermal flux was computed with accuracy comparable to that of ADEP, the transient flux solutions at other spatial points (not shown here) had large errors compared with the ADEP solutions. In regions 1,4,5 and 6 which had no perturbation, the neutron flux was expected to rise because of increased neutron diffusion from the perturbed regions 2 and 3. However, the closed-form analysis as outlined in Chapter 2 failed to account for this fact, thus resulting in inaccurate solutions in these regions as well as discontinuities along region interfaces.

Table 3: Peak thermal flux at  $x = 210$  cm versus time

Time (sec)	$\Delta t$ (sec)	ADEP				
		$5 \times 10^{-6}$	.002	.001	.0005	.0001
0.0		.392043	.392043	.392043	.392043	.392043
.01		.392598	.392715	.392660	.392632	.392610
.02		.394144	.394435	.394330	.394277	.394234
.03		.396533	.397122	.396970	.396894	.396832
.04		.399659	.400710	.400514	.400416	.400327

## CHAPTER 4

### CONCLUSIONS AND RECOMMENDATIONS

Two simple test problems have been examined to investigate the possible extension of the closed-form analysis to transient flux calculations. This chapter summarizes the findings in this study.

The first test case, the homogeneous slab with one energy group, has demonstrated that the space independent solution is not to be applied to a homogeneous region with the zero flux boundary condition. With no space independent solution, the closed-form analysis is then reduced to the eigenvector expansion technique.

The second test case, the six-region space dependent problem of the CANDU type, has identified some of the numerical difficulties associated with the closed-form analysis. First, it has indicated that the assumption of a separate exponential time dependence for each eigenmode solution will lead to a singularity matrix when the coefficients are normalized. Second, it has indicated that the closed-form analysis as presented in this study does not account for flux shape changes or neutron leakage across region interfaces. Thus, it can be concluded that the closed-form analysis as presented here is not satisfactory for transient flux calculations for a general space dependent problem. However, it should be pointed out that the cause of these numerical difficulties is mainly related to the procedure of using the region-dependent steady-state pseudo-bucklings throughout the transient, and not to the inclusion of the space independent solution.

The closed-form analysis must be modified and improved before it can be applied to a general space dependent problem. Some areas for modifications or improvements are suggested as follows:

- (a) The reactor kinetics equations should be multiplied by appropriate weighting functions and then integrated over the volume of the region considered. In this way, the neutron leakage across region interfaces can be accounted for. It should be noted however, that even such a procedure may not sufficiently account for flux tilts.<sup>(7)</sup>
- (b) A closer examination of the relation between the time constants of a reactor system and the eigenvalues obtained for different eigenmodes is required. This will lead to better approximations about the time dependence in the solution representation.
- (c) Instead of assuming the steady-state pseudo-bucklings throughout the transient, they may be updated periodically during the transient. This will necessarily involve recomputing the coefficients periodically. The feasibility of such a procedure has yet to be examined.

## APPENDIX A

### TEST PROBLEM DATA

The reactor configurations and parameters of the two test problems are listed here. All symbols have previously been defined in Section 1.2. The boundary condition for both problems is zero flux on the reactor outer boundary.

#### A.1 Homogeneous Slab

Number of energy groups = 1

Number of precursor groups = 1

Geometry: Bare homogeneous slab, 200 cm in width

Precursor Constants:

$$\lambda = .08 \text{ sec}^{-1}, \quad \beta = .0065, \quad x_{11} = 1.0.$$

Material Properties:

$$v = 2.2 \times 10^6 \text{ (cm/sec)}$$

$$D = .9338 \text{ cm}$$

$$v\Sigma_f = .00473 \text{ cm}^{-1}$$

$$\Sigma_a = .0045 \text{ cm}^{-1}$$

Initial Conditions:

Initial Spatial Shape: cosine

$$\text{Critical } k_{\text{eff}} = .99991419$$

Initial precursor concentrations are in equilibrium with the initial neutron flux distribution.

Perturbation:

$$\Delta \Sigma_a = -1.5 \text{ E-5}, -2. \text{ E-5}, -2.82 \text{ E-5}, -3.2 \text{ E-5}$$

## A.2 Six-Region Space Dependent Problem

Number of energy groups = 2

Number of precursor groups = 2

Geometry: One-dimensional, six-region reactor, 780 cm in width.

Precursor Constants:

$$\lambda_1 = .06297, \quad \beta_1 = .003213, \quad x_{11} = 1.0, \quad x_{21} = 0.$$

$$\lambda_2 = .6871, \quad \beta_2 = .004556, \quad x_{12} = 1.0, \quad x_{22} = 0.$$

Material Properties:

Region	Group	D	$v\Sigma_f$	$\Sigma_a$	$\Sigma_{1 \rightarrow 2}$
1,6	1	1.310	0.	.01021	.01018
	2	.8695	0.	.0002335	0.
2,5	1	1.264	.0002247	.008177	.007368
	2	.9328	.004523	.004031	0.
3,4	1	1.264	.0002217	.008163	.007368
	2	.9328	.004462	.004106	0.

Additional parameters for all regions are:

$$v_1 = 1.0 \times 10^7 \text{ (cm/sec)}, \quad v_2 = 3.0 \times 10^5 \text{ (cm/sec)}, \quad x_1 = 1.0, \quad x_2 = 0.$$

Initial Conditions:

$$\text{Critical } k_{\text{eff}} = 1.0084550$$

Initial configuration is made critical by dividing the production cross sections by the critical  $k_{\text{eff}}$ . The initial precursor concentrations are in equilibrium with the initial critical flux distribution.

Perturbation: Regions 2 and 3

$$\frac{\partial \Sigma_{a2}}{\partial t} = - 1.0 \times 10^4 \text{ (cm}^{-1} \text{ sec}^{-1}\text{)},$$

## APPENDIX B

### USER DESCRIPTION

The computer program for the first test problem is simple and has ample comments. No further explanation is necessary. The organization of the computer program for the second test problem is briefly described here. The program is organized specifically for this two-group problem and must be modified if a general multigroup problem is to be considered. Nevertheless, variable dimensioning is used to facilitate transfer of data. The code consists of the following program or sub-programs:

#### B.1 Program CANDU

The main purpose of this program is to read in data which define the geometry of the problem and to set up variable dimensions for the arrays. It also reads in the initial critical  $k_{eff}$  which has already been obtained by the finite difference code ADEP.

#### B.2 Subroutine MAIN

This subroutine is the core of the entire code. It first reads in the material properties, and specifies the spatial points where the transient fluxes are to be computed. Then it utilizes the subroutine STEDY to obtain the steady-state flux and precursor distributions. The transient is divided into small time steps. Within each step, the group 2 absorption cross sections in regions 2 and 3 are updated and the sub-

routine COEMAT is utilized to compute the eigenvalues, eigenvectors and to normalize the eigenvectors for each region except the reflectors. The subroutine MAIN then updates the coefficients. The coefficients for the reflector regions are found by considering continuity of flux and current. The solutions are printed by the subroutine RITE.

### B.3 Subroutine STEDY

This subroutine calculates the steady-state solutions at the specified points. Only one half of the core is actually considered since the steady-state neutron and precursor distributions are symmetric about the midplane of the reactor.

### B.4 Subroutine COEMAT

This subroutine sets up the coefficient matrices to compute the eigenvalues and eigenvectors as well as to normalize the eigenvectors. These eigenvectors are in fact the coefficients associated with the shape functions and are returned to the subroutine MAIN.

### B.5 Subroutine RITE

This subroutine prints and plots the steady-state and transient solutions at specified time intervals.

### B.6 Input Instructions

Card 1 Variables: NR, NG, ND, NPINT

Format: 10I5

NR = Number of regions

NG = Number of energy groups

ND = Number of delayed neutron precursor groups  
 NPINT = Number of interior spatial points at which  
 solutions are desired (points at region inter-  
 faces are not included).

Card 2 Variables: PFRAC, EFFK

Format: 4E15.8

PFRAC = Constant to permit adjustment of initial  
 power level

EFFK = Initial critical  $k_{eff}$

Card 3 Variables: (AL(I),BET(I),I=1,ND)

Format: 4E15.8

AL = Decay constant for  $i^{th}$  delayed precursor

BET = Delayed neutron fraction for  $i^{th}$  delayed  
 precursor

Card 4 Variables: (V(I),I=1, NG)

Format: 4E15.8

V = Speed of the energy group  $i$

Card 5 Variables: (D(I),I=1,NR\*NG)

Format: 4E15.8

D = Diffusion coefficient for group  $i$  in a region

Card 6 Variables: (SIG(I),I=1,NR\*NG)

Format: 4E15.8

SIG = Absorption cross section ( $\Sigma_a$ ) of group  $i$  in  
 a region

Card 7 Variables: (SIGF(I),I=1,NR\*NG)

Format: 4E15.8

SIGF = Production cross section ( $\nu\Sigma_f$ ) of group  $i$  in a region

Card 8 Variables: (SIGR(I), I=1, NR)

Format: 4E15.8

SIGR = Scattering cross section ( $\Sigma_{g' \rightarrow g}$ ) from group  
1 to group 2 in a region

Card 9 Variables: (NP(I), I=1, NR)

Format: 10I5

NP = Number of specified spatial points within a  
region i such that  $\sum_I NP(I) = NPINT$

Card 10 Variables: (DX(I), I=1, NR)

Format: 4E15.8

DX = Distance between spatial points in a region i.  
Uniform spacing is assumed.

APPENDIX C

PROGRAM LISTING

```

PROGRAM SLAB(INPUT,OUTPUT)
DIMENSION PHI(11),C(11),PSI(11),OMEGA(2),E1(2),E2(2)
REAL LAMECA
PRINT 600
PRINT 6005
READ 601, SIG,SIGF,D,V
PRINT 606, SIG,SIGF,D,V
READ 601, BET,LAMBDA
PRINT 607
PRINT 608, BET,LAMBDA
READ 601, WIDTH
PRINT 608, WIDTH
PI=ACOS(-1.0)
B=PI/WIDTH
BSQ=B*B
EFFK=SIGF/(SIG+D*BSQ)
SIGF=SIGF/EFFK
PRINT 610, EFFK
PRINT 615, SIGF
CONST1=1.
CONST2=SIGF*BET/LAMBDA
NPCINT=11
DX=10.
X=0.
T=0.
PRINT 625, T
PSI IS THE SHAPE FUNCTION
DC 50 N=1,NPCINT
PSI(N)=COS(B*X)
X=X+DX
PHI(N)=PSI(N)+CONST1
C(N)=PSI(N)+CONST2
CCONTINUE
PRINT 626
PRINT 627, (PHI(N),N=1,NPCINT)
PRINT 628
PRINT 627, (C(N),N=1,NPCINT)
READ 601, DSIG
PRINT 621, DSIG
SIG=SIG+DSIG
EFFK=SIGF/(SIG+D*BSQ)
PRINT 620, EFFK
X=(D*BSQ+SIG-SIGF)*V
X1=LAMBDA+(X+V*BET*SIGF)
X2=X*LAMECA
X=X1*X1-4.*X2
IF (X.LT. 0.) GO TO 550
X=SQRT(X)
OMEGA S ARE THE FREQUENCIES
OMEGA(1)=(X-X1)/2.

```

```

OMEGA(2)=- (X+X1)/2.
PRINT 715, OMEGA(1), OMEGA(2)
XK1=(LAMBDA+OMEGA(1))/(BET*SIGF)
XK2=(LAMBDA+OMEGA(2))/(BET*SIGF)
E1 AND E2 ARE THE COEFFICIENTS
E2(1)=(1.-XK2*CONST2)/(XK1-XK2)
E2(2)=(XK1+CONST2-1.)/(XK1-XK2)
E1(1)=XK1+E2(1)
E1(2)=XK2+E2(2)
X=E1(1)+E1(2)
PRINT 810, E1(1), E1(2), X, CCNST1
X=E2(1)+E2(2)
PRINT 820, E2(1), E2(2), X, CCNST2
TMAX=1.
DT=.02
TMAX=TMAX+1.E-8
NSTEP=TMAX/DT
DO 100 N=1, NSTEP
T=T+DT
PRINT 625, T
X1=0.
X2=0.
X1 AND X2 ARE THE AMPLITUDE FUNCTIONS
DO 60 N1=1, 2
X1=X1+E1(N1)*EXP(T*OMEGA(N1))
60 X2=X2+E2(N1)*EXP(T*OMEGA(N1))
X=0.
DO 70 N1=1, NPCINT
PHI(N1)=PSI(N1)*X1
C(N1)=PSI(N1)*X2
CALL PLOTFT(X, PHI(N1), 2)
70 X=X+DX
CONTINUE
PRINT 626
PRINT 627, (PHI(J), J=1, NPCINT)
PRINT 628
PRINT 627, (C(J), J=1, NPCINT)
100 CONTINUE
CALL OUTFLT
SIGF
550 PRINT 710
601 FCRMAT(5E15.8)
710 FCRMAT(//,*, COMPLEX ROOTS FOR OMEGA *,//)
715 FCRMAT(//,*, OMEGA1=*,E15.8,5X,*OMEGA2=*,E15.8,//)
600 FCRMAT(1FD,*, INFINITE SLAB, ONE ENERGY GROUP, ONE DELAYED GROUP*)
605 FCRMAT(//,*, SIG SIGF 0 V*,//)
606 FCRMAT(1X,4E15.8)
607 FCRMAT(//,*, BETA LAMBDA*,//)
608 FCRMAT(//,*, WIDTH OF SLAB=*,E15.8)
610 FCRMAT(//,*, CRITICAL KEFF=*,E15.8)
615 FCRMAT(//,*, CRITICAL SIGF=*,E15.8)
620 FCRMAT(//,*, KEFF=*,E15.8)
621 FCRMAT(//,*, CHANGE IN SIG=*,E15.8)
625 FCRMAT(//,*, FLUX AND PRECURSOR CONC. AT T=*,E15.8)
626 FCRMAT(//,*, FLUX*,//)
627 FCRMAT(1X,6E15.8)
628 FCRMAT(//,*, PRECURSOR CONC*,//)
810 FCRMAT(//,*, GROUP 1 CONSTANTS*,4E15.8)
820 FCRMAT(//,*, GROUP 2 CONSTANTS*,4E15.8)
END

```

```

PROGRAM CANDU(INPUT,CUTPUT)
COMMON AL(6),BET(6),BETA,BETM1,ND,NGPC,NRD2,NFINT,NIF,NIF2,FFRAC,E
ZFFK,Y(800)
COMMON/ADD/OMEGA(24),ALPHA(48),XK2(192),ITFFPHI(20),AMPSI(24),NOMEGA
1A,NALPHA,NIFPHI,DT,T
REAL ITFFPHI
C THE ARRAYS XK2(192) AND AMPSI(24) WERE NOT USED IN THE ANALYSIS
C READ 105, NR,NG,ND,NPINT
C PFRAC IS TO NORMALIZE PEAK THERMAL FLUX TO THE ADEP VALUE
C READ 110, PFRAC,EFFK
C READ 110, (AL(I),BET(I),I=1,ND).
BETA=0.
DO 5 I=1,ND
5 BETA=BETA+BET(I)
BETM1=1.-BETA
C SET ARRAY SIZE FOR VARIABLE DIMENSIONING
NIF=NR-1
NIF2=NIF+NIF
NRD2=NR/2
NGP=NG+NPINT
NDF=ND+NPINT
NGPC=NG+ND
NRNG=NR*NG
NRATIC=NR*(NGPC-1)*NGPC
NW=NGP+NCF
NU=NIF2*NGPD
NAMP=NR*NGPD*NGPD
NE=NR*NGPC
NF=NR*NGPC*NGPD*NG
NY=NGP+NDF+NG+3*NR+5*NRNG+NRATIC+NW+2*NU+NAMP+NE+NF
10 DO 10 I=1,NY
Y(I)=0.
NOMEGA=NR*NGPD
NALPHA=NR*NG+NGPC
NIFPHI=NIF+NGPC
11 DO 11 I=1,NOMEGA
OMEGA(I)=0.
12 DO 12 I=1,NALPHA
ALPHA(I)=0.
13 DO 13 I=1,NF
XK2(I)=0.
14 DO 14 I=1,NIFPHI
ITFFPHI(I)=0.
15 DO 15 I=1,NOMEGA
AMPSI(I)=0.
T=0.
N1=1
N2=1+NGP
N3=N2+NDF
N4=N3+NG

```

```

N6=N4+NRNG
N6=N5+NRNG
N7=N6+NRNG
N8=N7+NRNG
N9=N8+NRNG
N10=N9+NRNG
N11=N10+NRATIC
N12=N11+NR
N13=N12+NR
N14=N13+NW
N15=N14+NU
N16=N15+NU
N17=N16+NAMP
N18=N17+NE
N19=N18+NF
PRINT 120
PRINT 125, NR,NG,ND,NPINT,PFRAC,EFFK
PRINT 130
DC 20 I=1,ND
PRINT 135, I,AL(I),BET(I)
20 GCNTINUE
PRINT 140, N19
CALL HAIN(Y(N1),Y(N2),Y(N3),Y(N4),Y(N5),Y(N6),Y(N7),Y(N8),Y(N9),Y(
ZN10),Y(N11),Y(N12),Y(N13),Y(N14),Y(N15),Y(N16),Y(N17),Y(N18),NR,NG
Z,NGP,NDP,NRNG,NRATIC,NW,NU,NAMP,NE,NF)
105 FCRMAT(10I5)
110 FCRMAT(4E15.8)
120 FCRMAT(1H1,* REGIONS GROUPS DELAYED GROUPS INT.PCINTS POWER
1 FRACTION CRITICAL KEFF *,/)
125 FCRMAT(1X,4(I5,5X),2(E15.8,5X),////)
130 FCRMAT(* DELAYED GROUP DECAY CONSTANT DELAY FRACTION *,/)
135 FCRMAT(3X,I5,2(3X,E15.8),////)
140 FCRMAT(* MINIMUM ADDITIONAL FIELD LENGTH *, I10)
END

```

```

SUBROUTINE MAIN(PHI,C,V,D,SIG,SIGF,SIGR,BSQ,B,XK,NP,DX,W,U,DU,AMP,
1E,F,NR,NG,NGP,NCP,NRNG,NRATIO,NW,NU,NAMP,NE,NF)
COMMON/AL(6),BET(6),BETA,BETM1,ND,NGPC,NRO2,NFINT,NIF,NIF2,PFAC,E
ZFFK,Y(1)
COMMON/ACC/OMEGA(24),ALPHA(48),XK2(192),ITFPHI(20),AMPSI(24),NOMEG
1A,NALPHA,NIFPHI,DT,I
DIMENSION PHI(NGP),C(NCP)
DIMENSION V(NG),D(NRNG),SIG(NRNG),SIGF(NRNG),SIGR(NR),BSQ(NRNG),B(
1NRNG)
DIMENSION XK(NRATIO),NP(NR),DX(NR)
DIMENSION W(NW),U(NU),DU(NU),AMP(NAMP),E(NE),F(NF)
REAL ITFPHI
C REACTOR PARAMETERS
READ 505, (V(I),I=1,NG)
READ 505, (D(I),I=1,NRNG)
READ 505, (SIG(I),I=1,NRNG)
READ 505, (SIGF(I),I=1,NRNG)
READ 505, (SIGR(I),I=1,NR)
DC 5 I=1,NRNG
5 SIGF(I)=SIGF(I)/EFFK
PRINT 520
DC 20 L=1,NR
PRINT 525, L
DC 20 N=1,NG
L1=(L-1)*NG+N
IF (N.EC.NG) GO TO 10
PRINT 530, N,D(L1),SIG(L1),SIGF(L1),SIGR(L)
GC TO 20
10 PRINT 530, N,D(L1),SIG(L1),SIGF(L1)
20 CCCONTINUE
PRINT 535, V(1),V(2)
C REGION SET UP
READ 510, (NP(I),I=1,NR)
READ 505, (OX(I),I=1,NR)
PRINT 540
DC 50 L=1,NR
PRINT 545, L,NF(L),CX(L)
50 CCCONTINUE
C CALL STEADY SUBROUTINE TO COMPUTE STEADY STATE PSEUDO BUCKLINGS
C AND ASSIGN SHAPE FUNCTIONS AT EACH SPATIAL POINT
CALL STEADY(PHI,C,V,D,SIG,SIGF,SIGR,BSQ,B,XK,NP,DX,W,U,DU,AMP,E,F,N
1R,NG,NGP,NCP,NRNG,NRATIO,NW,NU,NAMP,NE,NF)
ITPR=1
DT=1.E-4
TMAX=4.E-2
TP=1.E-2
TMAX=1.E-8+TMAX
NSTEP=TMAX/DT
TF=TP-1.E-6
DC 450 ITRAN=1,NSTEP

```

```

T=T+DT
SIG(4)=SIG(4)-1.E-4*DT
SIG(6)=SIG(6)-1.E-4*DT
DC 300 L=2,NIF
CALL COEMAT(PHI,C,V,D,SIG,SIGF,SIGR,BSQ,B,XK,NP,DX,W,U,DU,AMP,E,F,
1NF,NG,NGP,NDP,NRNG,NRATIO,NW,NU,NAMP,NE,NF,L)
IL=(L-1)*NGPD*NGPD
IA0=(L-1)*NG*NGPD
IF0=IL*NG
IX0=(L-1)*(NGPC-1)*NG
DC 300 N=1,NGPC
IA=IA0
IF (N.NE. 1) IX0=IX0+1
IL=IL+2
X1=0.
DC 240 N2=1,NGPD
IA=IA+1
IF0=IF0+1
240 X1=X1+F(IF0)*EXP(DT*ALPHA(IA))
IF (N.EG. 1) XX1=X1
IF (N.NE. 1) GO TO 241
X2=AMP(IL-1)
X3=AMP(IL)
241 CCNTINUE
AMP(IL-1)=X2*X1
AMP(IL)=X3*X1
IF (N.EG. 1) GO TO 260
XK(IX0)=X1/XX1
260 CCNTINUE
IF (N.NE. 1) IX0=IX0+1
IF0=IF0+4
IL=IL+2
300 CCNTINUE
C COMPUTE AMPLITUDE FOR REFLECTOR REGIONS
C BY CONSIDERING CONTINUITY OF FLUX AND CURRENT
X1=AMP(17)+AMP(19)
AMP(2)=X1/U(2)
X1=AMP(21)+AMP(23)
X2=C(4)*AMP(22)+DU(6)+D(4)*AMP(24)*DU(8)
X3=U(2)+D(2)*DU(4)-D(2)*DU(2)+U(4)
AMP(6)=(X1+D(2)*DU(4)-X2*U(4))/X3
AMP(8)=(X2*U(2)-X1+D(2)*DU(2))/X3
X1=AMP(65)+AMP(67)
AMP(82)=X1/U(38)
X1=AMP(69)+AMP(71)
X2=C(10)*AMP(70)*DU(34)+D(10)*AMP(72)*DU(36)
X3=U(38)+C(12)*DU(40)-D(12)*DU(38)+U(40)
AMP(86)=(X1+D(12)*DU(40)-X2*U(40))/X3
AMP(88)=(X2*U(38)-X1+D(12)*DU(38))/X3
C COMPUTE FLUX AND PRECURSOR CONC. AT INTERIOR POINTS

```

```

IL=0
DC 350 L=1,NR
L1=(L-1)*NGPD*NGPD-NGPD
NN=NP(L)
DC 350 N1=1,NN
IL=IL+1
L3=(IL-1)*NGPD
L5=L1
DC 350 N2=1,NGPD
IL1=(N2-1)*NPINT+IL
L5=L5+NGPD
L2=L3
L1=L3
X1=0.
DC 340 N3=1,NGPD
L2=L2+1
L4=L4+1
340 X1=X1+AMP(L2)*W(L4)
350 PHI(IL1)=X1*PFRAC
C CCM COMPUTE FLUX AND PRECURSOR CONC. AT REGION BOUNDARIES
L0=0
L1=NGPD*NGPD
DC 400 L=1,NIF
L0=L0+NGPD
IL1=L
IF (L.NE.NRD2) GO TO 360
L0=L0-NGPD
360 L1=L1-NGPD*NGPD
CCCONTINUE
DC 390 N=1,NGPD
L2=L0
X1=0.
DC 380 N1=1,NGPD
L2=L2+1
L1=L1+1
380 X1=X1+AMP(L1)*U(L2)
ITFFPHI(IL1)=X1*PFRAC
390 IL1=IL1+NIF
400 L0=L0+NGPD
C TC APPROXIMATE PRECURSOR CONC. AT REFLECTOR BOUNDARIES
X=4./7.
ITFFPHI(11)=ITFFPHI(11)*X
ITFFPHI(15)=ITFFPHI(15)*X
ITFFPHI(16)=ITFFPHI(16)*X
ITFFPHI(20)=ITFFPHI(20)*X
II=I/TP
IF(II.LT.ITPR) GO TO 450
CALL RITE(PHI,C,V,O,SIG,SIGF,SIGR,BSQ,B,XK,NP,DX,W,U,DU,AMP,E,F,NR
1,NG,NGP,NCP,NRNG,NRATIO,NW,NU,NAMP,NE,NF)
ITPR=ITPR+1
450 CCCONTINUE
RETURN
505 FCRMAT(4E15.8)
510 FCRMAT(10I5)
520 FCRMAT(* REGION GROUP 0 SIG SIGF
Z SIGR +,/)
525 FCRMAT(1X,I3)
530 FCRMAT(10X,I3,5X,4E15.8)
535 FCRMAT(//,*,V1=*,E15.8,5X,*,V2=*,E15.8,/)
540 FCRMAT(///,*,REGION NP DX +,/)
545 FCRMAT(1X,2(I3,5X),E15.8)
END

```

```

SUBROUTINE STUDY (PHI,C,V,D,SIG,SIGF,SIGR,BSQ,B,XK,NP,DX,W,U,DU,AMP
Z,E,F,NR,NG,NGP,NCP,NRNG,NRATIO,NW,NU,NAMP,NE,NF)
COMMON AL(6),BET(6),BETA,BETM1,ND,NGPC,NRD2,NPINT,NIF,NIF2,PFRAC,E
ZFFK,Y(1)
COMMON/ACC/OMEGA(24),ALPHA(48),XK2(192),ITFFPHI(20),AMPSI(24),NOMEG
1A,NALPHA,NIFPHI,CT,I
DIMENSION PHI(NGP),C(NGP)
DIMENSION V(NG),D(NRNG),SIG(NRNG),SIGF(NRNG),SIGR(NR),BSQ(NRNG),B(
1NRNG)
DIMENSION XK(NRATIO),NP(NR),DX(NR)
DIMENSION W(NW),U(NU),DU(NU),AMP(NAMP),E(NE),F(NF)
DIMENSION A(9,9),P(9,1),WKAREA(108)
REAL ITFFPHI

```

```

C ONLY HALF OF THE CORE IS CONSIDERED FOR STEADY STATE DISTRIBUTION
C FOR TWO GROUP ANALYSIS ONLY

```

```

NPDONE=0
K=0
K1=NW-NGPD
L1=0
L2=0
DO 200 L=1,NRD2
IL4=(NR+1-2*L)*(NGPD-1)*NG
NPDONE=NPDONE+NP(L)*NGPD
L1=(L-1)*NG+1
L2=L1+1
X1=D(L1)*D(L2)
X2=D(L1)*SIG(L2)+D(L2)+(SIG(L1)-SIGF(L1))
X3=SIG(L2)*(SIG(L1)-SIGF(L1))-SIGR(L)*SIGF(L2)
PRINT 700, L, X1, X2, X3
IF (X3 .EQ. 0.) GO TO 660
X4=X2*X2-4*X1*X3
IF (X4 .LT. 0.) GO TO 670
X1=X1+X1
BSQ(L1)=(SQRT(X4)-X2)/X1
BSQ(L2)=-(SQRT(X4)+X2)/X1
IF (L .EQ. 1) BSQ(L1)=-SIG(L1)/D(L1)
IF (L .EQ. 1) BSQ(L2)=-SIG(L2)/D(L2)
X1=ABS(BSQ(L1))
X2=ABS(BSQ(L2))
B(L1)=SQRT(X1)
B(L2)=SQRT(X2)
L3=L3+1
XK(L3)=SIGR(L)/(D(L2)*BSQ(L1)+SIG(L2))
IL5=IL4+L3
XK(IL5)=XK(L3)
PRINT 705, L3, XK(L3)
L3=L3+1
IF (L .EQ. 1) GO TO 20
XK(L3)=SIGR(L)/(D(L2)*BSQ(L2)+SIG(L2))
IL5=IL4+L3

```

```

XK(L5)=XK(L3)
PRINT 705, L3, XK(L3)
PRINT 810
20 L3=L3+NG*NG
DC 150 N=1,NG
X1=B(L1)*CX(L)
IF (BSQ(L1) .EQ. 0.) GO TO 660
IF (L .EQ. 1) GO TO 50
L4=L4+1
U(L4)=1.
DU(L4)=0.
L4=L4+1
U(L4)=0.
DU(L4)=B(L1)
50 IF (BSQ(L1) .LT. 0.) GO TO 100
NN=NP(L)
DC 60 J=1,NN
X=(J-.5)*X1
K=K+1
K1=K1+1
W(K)=CCS(X)
W(K1)=W(K)
PRINT 815, K, K1, W(K)
K=K+1
K1=K1+1
W(K)=SIN(X)
W(K1)=W(K)
PRINT 815, K, K1, W(K)
60 K=K+NG
K1=K1-NG-NGPD
X=X+DX(L)*.5*B(L1)
L5=L5+1
U(L5)=CCS(X)
DU(L5)=-B(L1)*SIN(X)
L5=L5+1
U(L5)=SIN(X)
DU(L5)=B(L1)*CCS(X)
GO TO 140
100 CCNTINUE
NN=NP(L)
DC 110 J=1,NN
X=(J-.5)*X1
K=K+1
K1=K1+1
W(K)=COS(X)
W(K1)=W(K)
PRINT 815, K, K1, W(K)
K=K+1
K1=K1+1
W(K)=SINH(X)

```

```

W(K1)=W(K)
PRINT 815, K, K1, W(K)
K=K+NG
110 K1=K1-NG-NGPD
X=X+CX(L)*.5*B(L1)
L5=L5+1
U(L5)=CCSF(X)
OU(L5)=B(L1)*SINH(X)
L5=L5+1
U(L5)=SINH(X)
140 DU(L5)=B(L1)*COSH(X)
K=K-(NP(L)-1)*NGPD-NG
K1=K1+NP(L)*NGPD+NG
150 L1=L1+1
L4=L5
L5=L5+NGPD
K=NPDONE
K1=NW-K-NGPD
200 CCNTINUE
C DEFINE XK FOR THE PRECURSORS
DC 203 L=2, NIF
IL1=(L-1)*NG+1
IL2=IL1+1
IX0=(L-1)*(NGPD-1)+NG
DC 202 N1=1, NG
IX0=IX0+1
IX1=IX0+NG
DC 202 N2=1, ND
XK(IX1)=BET(N2)*(SIGF(IL1)+SIGF(IL2)+XK(IX0))/AL(N2)
202 IX1=IX1+NG
203 CCNTINUE
PRINT 829
IL1=1
IL2=6
DC 204 L=1, 6
PRINT 830, (XK(J), J=IL1, IL2)
IL1=IL1+6
IL2=IL2+6
204 C SIMILARLY DEFINE SHAPE FUNCTIONS ND THEIR DERIVATIVES AT REGION INTERF
C FOR THE RIGHT HALF CORE
IL1=NIF*NGPD
DC 205 I=1, NIF
IL2=(NIF-I)*NGPD
DC 205 N=1, NGPD
IL1=IL1+1
IL2=IL2+1
U(IL1)=U(IL2)
OU(IL1)=-OU(IL2)
IF (I.EC. 1) OU(IL1)=OU(IL2)
205 CCNTINUE

```

C SIMILARLY DEFINE BUCKLINGS FOR THE RIGHT HALF CORE

```

L1=NRD2*NG
L2=L1
DC 207 I=1,NRD2
L2=L2-2
DC 206 II=1,NG
L1=L1+1
L2=L2+1
BSQ(L1)=BSQ(L2)
206 B(L1)=B(L2)
207 L2=L2-2
PRINT 708
PRINT 709, (BSQ(N), N=1,MRNG)
PRINT 711
PRINT 710, (U(N),N=1,NU)
PRINT 712
PRINT 710, (DU(N), N=1,NU)
DC 210 I=1,9
P(I)=0.
DC 210 J=1,9
210 A(I,J)=0.
A(1,1)=XK(1)*U(2)
A(2,1)=C(1)*DU(2)
A(3,1)=C(2)*XK(1)*DU(2)
P(1)=-U(4)
P(3)=-C(2)*DU(4)
J=1
L4=NGPD
L3=NG*(NGPD-1)
DC 250 I=1,NG
L3=L3+1
DC 250 II=1,NG
L4=L4+1
J=J+1
A(1,J)=-XK(L3)*U(L4)
A(2,J)=-C(3)*DU(L4)
A(3,J)=-C(4)*XK(L3)*DU(L4)
L5=L4+NGPD
A(4,J)=U(L5)
A(5,J)=XK(L3)*U(L5)
A(6,J)=C(3)*DU(L5)
250 A(7,J)=C(4)*XK(L3)*DU(L5)
L3=L3+NG*NC
L4=L5
DC 300 I=1,NG
L3=L3+1
DC 300 II=1,NG
L4=L4+1
J=J+1
A(4,J)=-L(L4)

```

```

A(5,J)=-XK(L3)*U(L4)
A(6,J)=-C(5)*DU(L4)
A(7,J)=-D(6)*XK(L3)*DU(L4)
L5=L4+NGPD
300 A(8,J)=C(5)*DU(L5)
A(9,J)=D(6)*XK(L3)*DU(L5)
ME=1
N7=9
I7=9
ICGT=0
CALL LEQT2F(A,MB,NA,IA,P,ICGT,WKAREA,IER)
IF (IER .GE. 128) GO TO 880
L=1
AMP(2)=P(1)
AMP(6)=XK(1)*AMP(2)
AMP(8)=1.
NGP1=NG+1
J=1
DC 400 I=1,2
L=L+1
L1=(L-1)*NG+1
L2=L1+1
IL=(L-1)*NGPD*NGPD
L3=(L-1)*(NGPD-1)*NG+1
DC 400 II=1,NGPD
J=J+1
IL=IL+1
IL1=IL+NGPD
AMP(IL)=P(J)
IF (II .EQ. NGP1) L3=L3+1
AMP(IL1)=XK(L3)*AMP(IL)
X1=SIGF(L1)*AMP(IL)+SIGF(L2)*AMP(IL1)
IL2=IL1
DC 400 IJ=1,NR
X2=BET(IJ)/AL(IJ)
IL2=IL2+NGPD
400 AMP(IL2)=X1*X2
DO 450 L=1,NR2
IL1=(L-1)*NGPD*NGPD
ILO=(NR+1-2*L)*NGPD*NGPD
DC 450 I=1,NGPD
IL1=IL1+1
IL2=IL1-NGPD
DC 450 II=1,NGPD
IL2=IL2+NGPD
IL3=IL2+ILO
450 AMP(IL3)=AMP(IL2)
IL=0
DC 500 L=1,NR
L1=(L-1)*NGPD*NGPD-NGPD

```

```

NN=NP(L)
DC 500 N=1,NN
IL=IL+1
L3=(IL-1)*NGPD
L5=L1
DC 500 K=1,NGPD
IL1=(K-1)*NPINT +IL
L5=L5+NGPC
L2=L5
L4=L3
DC 500 KK=1,NGPD
L2=L2+1
L4=L4+1
500 PHI(IL1)=PHI(IL1)+AMP(L2)*W(L4)*PFRAC
C COMPUTE INITIAL FLUXES AND PRECURSOR CONC. AT REGION INTERFACES
C THESE ARE STORED GROUP BY GROUP AND WITHIN A GROUP, POINT BY POINT
L0=0
L1=NGPD*NGPD
DC 560 L=1,NIF
L0=L0+NGPC
IL1=L
IF (L .NE. NR02) GO TO 535
L0=L0-NGPC
L1=L1-NGPC*NGPC
535 CONTINUE
DC 550 N=1,NGPD
L2=L0
DC 540 N1=1,NGPD
L2=L2+1
L1=L1+1
540 ITFFPHI(IL1)=ITFFPHI(IL1)+AMP(L1)*U(L2)*PFRAC
550 IL1=IL1+NIF
560 L0=L0+NGPC
X=4./7.
ITFFPHI(11)=ITFFPHI(11)*X
ITFFPHI(15)=ITFFPHI(15)*X
ITFFPHI(16)=ITFFPHI(16)*X
ITFFPHI(20)=ITFFPHI(20)*X
CALL RITE(PHI,C,V,D,SIG,SIGF,SIGR,BSQ,B,XK,NP,DX,W,U,DU,AMP,E,F,NR
1,NG,NGP,NCP,NRNG,NRATIO,NW,NU,NAMP,NE,NF)
RETURN
660 PRINT 730
STOP
670 PRINT 740
STOP
680 PRINT 750
STOP
700 FCRMAT(//,* REGION *,I3,* X1= *,E15.8,* X2= *,E15.8,* X3= *,E
Z15.8)
705 FCRMAT(//,* L3= *,I5,* X RATIO= *, E15.8)

```

```
708 FCRMAT (//, * PSEUDO-BUCKLINGS *, //)
709 FCRMAT (1X, 2E15.8)
710 FCRMAT (//, 4(5X, E15.8))
711 FCRMAT (//, * SHAPE FUNCTIONS AT INTERFACES *, //)
712 FCRMAT (//, * DERIVATIVES OF SHAPE FUNCTIONS AT INTERFACES *, //)
730 FCRMAT (* ONE ROOT OF BSQ=0 *)
740 FCRMAT (* COMPLEX ROOTS IN BSQ *)
750 FCRMAT (* TERMINAL ERROR IN A MATRIX *)
810 FCRMAT (//, * LEFT CORE RIGHT CORE *, //)
815 FCRMAT (2(7X, I3), 10X, E15.8)
825 FCRMAT (//, * XRATIC *, //)
830 FCRMAT (5X, 6E15.8)
ENC
```

```

SUBROUTINE COEMAT(PHI,C,V,D,SIG,SIGF,SIGR,BSQ,B,XK,NP,DX,W,U,DU,AM
1P,E,F,NR,NG,NGF,NDP,NRNG,NRATIO,NW,NU,NAMP,NE,NF,L)
CCMNCN AL(6),BET(6),BETA,BETH1,ND,NGPC,NRD2,NPINT,NIF,NIF2,PFRAC,E
ZFFK,Y(1)
CCMNCN/ACE/CMEGA(24),ALPHA(48),XK2(192),ITFPHI(20),AMPSI(24),NCEG
1A,NALPHA,NIFPHI,DT,I
DIMENSION PHI(NGP),C(NDP)
DIMENSION V(NG),D(NRNG),SIG(NRNG),SIGF(NRNG),SIGR(NR),BSQ(NRNG),B(
1NRNG)
DIMENSION XK(NRATIO),NP(NR),DX(NR)
DIMENSION W(NW),U(NU),DU(NU),AMP(NAMP),E(NE),F(NF)
DIMENSION A(4,4),Z(4,4),WK(24),EVALUE(4)
DIMENSION AA(16,7),XB(16,1),XU(16,9),XL(64)
COMPLEX Z,EVALUE

```

C THIS SUBROUTINE IS NOT UTILIZED BY REFLECTOR REGIONS  
C COMPUTE EIGENVALUES AND EIGENVECTORS FOR ONLY THE FIRST EIGENMODE

```

DC 10 I=1,NGPD
DC 10 II=1,NGPC
10 A(I,II)=0.
IL=(L-1)*NG+1
IL1=IL+1
A(1,1)=V(1)*(SIGF(IL)*BETH1-SIG(IL))
A(2,2)=-V(2)*SIG(IL1)
A(3,3)=-AL(1)
A(4,4)=-AL(2)
A(1,2)=V(1)+BETH1*SIGF(IL1)
A(1,3)=V(1)*AL(1)
A(1,4)=V(1)*AL(2)
A(2,1)=V(2)*SIGR(L)
A(3,1)=BET(1)*SIGF(IL)
A(3,2)=BET(1)*SIGF(IL1)
A(4,1)=BET(2)*SIGF(IL)
A(4,2)=BET(2)*SIGF(IL1)
NGPCP1=NGPC+1
NGPCM1=NGPC-1
NGPCSQ=NGPC*NGPC
NLC=NGPC-1
NUC=NLC
NS=NLC+NUC+1
LQ=(L-1)*NG*NGPD
L1=LQ*NGPC
Ll=L1+1
L1=L1+1
IL1=(L-1)*NG+1
IL2=IL1+1
IL3=IL1
IL3=(L-1)*NGPCM1*NG
IF0=(L-1)*NGPD*NG*NGPD
IF (BSQ(IL3) .EQ. 0) GO TO 410
X1=V(1)*C(IL1)*BSQ(IL3)

```

```

XZ=V(2)*C(IL2)*BSQ(IL3)
A(1,1)=A(1,1)-X1
A(2,2)=A(2,2)-X2
CALL EIGRF(A,NGPD,4,2,EVALUE,Z,4,WK,IER)
A(1,1)=A(1,1)+X1
A(2,2)=A(2,2)+X2
IL0=IL0+1
DC 70 I=1,NGPD
ALPHA(L0)=EVALUE(I)
70 L0=L0+1
   IL3=IL3+1
   DC 80 I=1,NGPDSQ
   XE(I)=0.
   DC 80 II=1,NS
80 AA(I,II)=0.
   ILL=NGPDSQ-NGPCP1
   L3=NLC
   IX1=0
   DC 120 I=1,ILL,NGPDF1
   L4=L3+1
   L5=L3+NGFC
90 DC 90 II=L4,L5
   AA(I,II)=1.
   IX1=IX1+1
   IX2=IX1+1
   DC 100 IX0=1,NGPD
   IX=IX0+I
100 AA(IX,L3)=Z(IX2,IX0)
   AA(IX,L5)=-Z(IX1,IX0)
120 L3=L3-1
   CCNTINUE
   IX=IX+1
130 DC 130 IX0=1,NGPD
   AA(IX,IX0)=1.
   XE(1)=1.
   XE(6)=XK(IL3)
   XE(11)=XK(IL3+2)
   XE(16)=XK(IL3+4)
CALL LEQT2B(AA,NGPDSQ,NLC,NUC,16,XB,1,16,0,XU,16,XL,IER)
IF (IER .EQ. 129) GC TC 420
K=0
IF1=IF0
DC 150 I=1,NGPD
DC 140 II=1,NGPD
K=K+1
IF1=IF1+1
140 F(IF1)=XE(K)
150 IF1=IF1+NGPC
IF0=IF0+NGPD
RETURN
410 PRINT 610
610 FCRMAT(//,* ONE RCCT OF BSQ =0 *,//)
STOP
420 PRINT 620
620 FCRMAT(//,* SINGULARITY COEFF. MATRIX,SPACE-DEPENDENT PART *,//)
STOP
END

```

```

SUBROUTINE RITE(PHI,C,V,C,SIG,SIGF,SIGR,BSQ,B,XK,NP,DX,H,U,DU,AMP,
1E,F,NR,NG,NGP,NOP,NRNG,NRATIO,NH,NU,NAMP,NE,NF)
COMMON AL(6),SET(6),BETA,BETM1,NO,NGPD,NRD2,NFINT,NIF,NIF2,FFRAC,E
ZFFK,Y(1)
COMMON/ADD/OMEGA(24),ALPHA(48),XK2(192),ITFPHI(20),AMPSI(24),NOMEG
1A,NALPHA,NIFPHI,CT,T
DIMENSION PHI(NGP),C(NOP)
DIMENSION V(NG),D(NRNG),SIG(NRNG),SIGF(NRNG),SIGR(NR),BSQ(NRNG),B(
1NRNG)
DIMENSION XK(NRATIO),NP(NR),DX(NR)
DIMENSION W(NW),U(NU),DU(NU),AMP(NAMP),E(NE),F(NF)
REAL ITFPHI
PRINT 540, T
IL1=1
IL2=NFINT
DC 100 N=1,NGPD
PRINT 550,N
PRINT 555, (PHI(IL),IL=IL1,IL2)
100 IL1=IL1+NFINT
IL2=IL2+NFINT
PRINT 560
IL1=1
IL2=NIF
DC 120 N=1,NGPD
PRINT 550, N
PRINT 555, (ITFPHI(IL),IL=IL1,IL2)
120 IL1=IL1+NIF
IL2=IL2+NIF
N1=0
DC 200 L=1,NR
NN=NP(L)
DC 150 N=1,NN
N1=N1+1
X=(N1-.5)*30.
N2=N1+NPINT
Y1=PHI(N1)
Y2=PHI(N2)
CALL PLOTFT(X,Y1,2)
CALL PLOTFT(X,Y2,4)
150 CCNTINUE
IF (L.EQ.NR) GO TO 200
X=X+.5*30.
Y1=ITFPHI(L)
Y2=ITFPHI(L+NIF)
CALL PLOTFT(X,Y1,44)
CALL PLOTFT(X,Y2,9)
200 CCNTINUE
CALL OUTPLT
CALL PRINTW(21HFAST AND THERMAL FLUX)
CALL OUTLIN

```

```

540 RETURN
550 FCRMAT(1H1,* FLUX AND PRECURSOR CONC. AT T=*,E15.8)
555 FCRMAT(//,*, GROUP*,I2,/)
559 FCRMAT(1X,8E15.8)
560 FCRMAT(1X,5E15.8)
FCRMAT(//,*, FLUX AND PRECURSOR CONC. AT INTERFACES *,//)
END

```

INPUT DATA

6	2	26				
.170608		1.0084550				
6.297	E-2	3.213	E-3	6.871	E-1	4.556
1.0	E+7	3.0	E+5			E-3
1.310		.8695		1.264		.9328
1.264		.9328		1.264		.9328
1.264		.9328		1.310		.8695
1.021	E-2	2.335	E-4	8.177	E-3	4.031
8.163	E-3	4.106	E-3	8.163	E-3	4.106
8.177	E-3	4.031	E-3	1.021	E-2	2.335
0.		0.		2.247	E-4	4.523
2.217	E-4	4.462	E-3	2.217	E-4	4.462
2.247	E-4	4.523	E-3	0.		0.
1.018	E-2	7.368	E-3	7.368	E-3	7.368
7.368	E-3	1.018	E-2			
3	4	6	4	3		
	30.		30.		30.	
	30.		30.		30.	

## REFERENCES

1. W.J. Garland and A.A. Harms, "A Closed-Form Analysis for Space Dependent Nuclear Reactor Transients," *Journal of Nuclear Energy*, Vol.26,p.241 (1972).
2. W.H. Reed and K.F. Hansen, "Alternating-Direction Methods for the Reactor Kinetics Equations," *Nucl. Sci. Eng.* 41, 431 (1970).
3. A.L. Wight, K.F. Hansen, and D.R. Ferguson, "Application of Alternating-Direction Implicit Methods to the Space-Dependent Kinetics Equations," *Nucl. Sci. Eng.* 44, 239 (1971).
4. D.R. Ferguson and K.F. Hansen, "Solution of the Space-Dependent Reactor Kinetics Equations in Three Dimensions," *Nucl. Sci. Eng.* 51, 189 (1973).
5. W.J. Garland, A.A. Harms, and J. Vlachopoulos, "Space-Time Nuclear Reactor Analysis by Temporal Transformation," *Nucl. Sci. Eng.* 55, 119 (1974).
6. A.A. Harms, W.J. Garland, W.A. Pearce, M.F. Harding, O.A. Trojan, and J. Vlachopoulos, "Multiple Temporal-Mode Analysis for Three Dimensional Reactor Dynamics," *Proceedings of the Joint NEACRP/CSNI Specialists' Meetings on New Developments in Three Dimensional Neutron Kinetics and Review of Kinetics Benchmark Calculations*, p.73 (March, 1975).
7. W.M. Stacey, Jr., Space Time Nuclear Reactor Kinetics, Chapter 1, Academic Press, New York (1969).
8. P.F. Zweifel, Reactor Physics, Chapters 3 and 4, McGraw Hill, New York (1973).

9. F.B. Hildebrand, Methods of Applied Mathematics, Prentice Hall, Englewood Cliffs, N.J. (1965).
10. R.S. Denning, "ADEP, One- and Two-Dimensional Few Group Kinetics Code," BMI-1911 (July, 1971).